Hybrid FM-Polynomial Phase Signal Modeling: Parameter Estimation and Cramér–Rao Bounds

Fulvio Gini and Georgios B. Giannakis, *Fellow, IEEE*

***Abstract*— Parameter estimation for a class of nonstationary signal models is addressed. The class contains combination of a polynomial-phase signal (PPS) and a frequency-modulated (FM) component of the sinusoidal or hyperbolic type. Such signals appear in radar and sonar applications involving moving targets with vibrating or rotating components. A novel approach is proposed that allows us to decouple estimation of the FM parameters from those of the PPS, relying on properties of the multilag high-order ambiguity function (ml-HAF). The accuracy achievable by any unbiased estimator of the hybrid FM-PPS parameters is investigated by means of the Cramér–Rao lower bounds (CRLB's). Both exact and large sample approximate expressions of the bounds are derived and compared with the performance of the proposed methods based on Monte Carlo simulations.**

***Index Terms*—Ambiguity function, performance bounds, signal modeling, sonar radar.**

I. Introduction and Problem Statement

THIS PAPER concerns parameter estimation of a hybrid frequency-modulated (FM) and polynomial-phase signal (PPS) from a finite number of noisy observations. The discrete-time model of the hybrid FM-PPS signal of interest is

$$\begin{aligned} s(n) &= \rho\, e^{j\phi_{\rm FM}(n)}\, e^{j\phi_{\rm PPS}(n)} \\ &= \rho\, e^{j\phi_{\rm FM}(n)}\, \exp(j2\pi \sum_{i=0}^{M} a_i n^i/i!) \end{aligned} \tag{1}$$

where $\{a_i\}_{i=0}^{M}$ are the PPS coefficients, ρ denotes a constant (perhaps unknown) amplitude, and M is the PPS order. Note that $\exp[j\phi_{\rm PPS}(n)]$ corresponds to a complex harmonic when $M=1$ and a chirp (or linear FM) when $M=2$. In (1), the term $\exp[j\phi_{\rm FM}(n)]$ represents a *sinusoidal FM* signal when $\phi_{\rm FM}(n) = 2\pi b \sin(\omega_0 n + \phi_0)$, where $b>0$ is the so-called modulation index, and ω_0 and ϕ_0 are the radian frequency and initial phase, respectively. Alternatively, the model (1) includes a *hyperbolic FM* signal when $\phi_{\rm FM}(n) = 2\pi\gamma \ln(n)$, where γ is a parameter that controls the decreasing rate of the instantaneous frequency $f_I(n) = \gamma/n$ [3], [16].

Manuscript received January 27, 1997; revised August 21, 1998. This work was supported by the Office of Naval Research under Grant N00014-93-1-0485. The associate editor coordinating the review of this paper and approving it for publication was Prof. James Bucklew.

F. Gini is with the Department "Ingegneria dell'Informazione," University of Pisa, Pisa, Italy (e-mail: gini@iet.unipi.it).

G. B. Giannakis was with the Department of Electrical Engineering, University of Virginia, Charlottesville, VA 22903-2442 USA (e-mail: georgios@virginia.edu). He is now with the Department of Electrical Engineering, University of Minnesota, Minneapolis, MN 55455 USA.

Publisher Item Identifier S 1053-587X(99)00733-3.

Signals described by (1) are encountered in many engineering applications such as radar, sonar, acoustics, and optics. One of the primary motivations for studying PPS comes from Doppler radar applications. When the target is moving, the samples taken at the matched filter output of a pulsed radar can be modeled as a discrete-time PPS (see e.g., [21, pp. 58–65]). The polynomial coefficients $\{a_i\}$ are related to the kinematic parameters of the moving target [21, p. 59], [19, p. 403]. The problem of PPS parameter estimation has been thoroughly investigated. The high-order instantaneous moment (HIM) and its Fourier transform [the high-order ambiguity function (HAF), which was introduced by Peleg and Porat in [18] (see also [19, ch. 12])], have provided a simple albeit suboptimum algorithm for estimating the PPS coefficients recursively. HIM and HAF offer good alternatives to the computationally intensive maximum likelihood (ML) approach. Additional results on constant, (deterministic or random) time-varying amplitude PPS can be found in [14], [20], [22], and [26]. Recently, a more general approach called product multilag HAF (ml-HAF) [2] has been devised to improve performance of the HAF, both in terms of removing identifiability problems as well as in terms of increasing signal-to-noise ratio. Cramér–Rao lower bounds (CRLB's) for the parameter estimates of a PPS observed in additive and multiplicative noise are derived in [25].

Signals arising from moving targets however, cannot always be modeled as a pure PPS. For example, sinusoidal FM signals arise from vibrating targets [12], [28] or rotating parts of the target [7], [15]. Specifically, suppose that an oscillating object is illuminated with an incident laser, RF, or acoustic wave, and the vibration velocity is slower than the wave speed, whereas the vibration frequency is considerably lower than the carrier frequency. The backscattered signal can then be modeled as a pure-tone FM process [12], [28]. Sinusoidal FM also appears as a result of the so-called jet engine modulation (JEM) phenomenon [7]. JEM occurs when a radar observes a jet airplane at an aspect angle that scatters electromagnetic radiation from the moving parts of the compressor and blade assembly of the engine. An accurate parametric model describing the JEM process has been proposed in [7], where it is validated with real data collected by a pulse-Doppler radar system. A similar model appears in helicopter recognition problems, where the helicopter return is characterized by sinusoidal FM signals due to the modulation introduced by the rotating blades (see [15] and references therein). The problem of sinusoidal FM parameter estimation and, especially, the challenging task of

estimating the modulation index have been studied extensively in the literature [12], [27], [28], particularly with the purpose of target classification [3], [7], [15]. When both of these effects (motion and vibration/rotation) are present, the noise-free backscattered signal obeys (1), and the estimation algorithms proposed for a pure sinusoidal FM are no more appropriate. On the other hand, when an FM component is also present, we cannot estimate the PPS parameters from the HAF as described in [18] or [26].

Another case of primary importance in sonar applications concerns backscattering from a moving target of a hyperbolic FM signal [3], [17]. Hyperbolic FM signals are used in sonar signal processing because they are Doppler-invariant [17], which means they are similar to the signals used by bats and dolphins for ecolocation [16]. When the target is maneuvering, PPS modulation is superimposed to the transmitted narrowband signal due to the motion, and again, the observed discrete-time signal can be modeled as in (1). In [16], a method for estimating jointly the hyperbolic parameter γ and the first-order parameter a_1 is proposed. It is based on phase unwrapping and linear fitting, but higher order PPS parameters were not considered, and the allowable range of γ was relatively small (e.g., $|\gamma| < 1.7$ when $a_1 = 0$).

The problem of joint estimation of the PPS and FM parameters has not been investigated. The main contribution of this paper is to show that the HIM and the HAF offer effective tools for parameter estimation, even when the observed data are not modeled as a pure PPS but when a nonlinear (sinusoidal or hyperbolic) FM component is also present.

The rest of the paper is organized as follows. In the next section, the relationships between the FM-PPS parameters and the multilag HIM are derived in the noise-free case. These relationships are important because they suggest a way to separate the problem of FM parameter estimation from the PPS one, with noticeable computational savings with respect to the ML approach. Both wideband and narrowband sinusoidal FM are considered. In Section III, the parameter estimation algorithms are described. In Section IV, CRLB expressions are derived for the hybrid FM-PPS model and for both sinusoidal and hyperbolic components. Computer simulations are also included to analyze the performance of various algorithms. Finally, conclusions are reported in Section V.

II. The Multilag HIM of Hybrid FM-PPS Signals

The problem considered in this paper is the joint estimation of the PPS parameters $\boldsymbol{\theta}_{\rm PPS} := [a_0 \cdots a_M]^T$, ^{T} denoting transpose, and those $\boldsymbol{\theta}_{\rm FM}$ of the FM component from a single record of N noisy observations[1] $\{x(n) = s(n) + v(n)\}_{n=0}^{N-1}$. The additive noise $v(n)$ is assumed stationary and mixing in the sense of [8, p. 25].

If the distribution of $v(n)$ is known [e.g., $v(n)$ is Gaussian or i.i.d. non-Gaussian with known parameters], then ML estimation of $(\boldsymbol{\theta}_{\rm PPS}, \boldsymbol{\theta}_{\rm FM})$ is possible but computationally demanding. If $v(n)$ is zero-mean, complex white-Gaussian with variance σ_v^2, the log-likelihood function

$$\Lambda(\boldsymbol{\theta}) = -\frac{1}{\sigma_v^2}\sum_{n=0}^{N-1}\left|x(n) - \rho \times \exp(j2\pi\sum_{i=0}^{M} a_i n^i/i!)\,\exp^{j\phi_{\rm FM}(n)}\right|^2 \quad (2)$$

can be maximized w.r.t. $\boldsymbol{\theta} := [\boldsymbol{\theta}_{\rm PPS}^T\,\boldsymbol{\theta}_{\rm FM}^T]^T$ to yield the parameter estimator

$$\hat{\boldsymbol{\theta}} = \arg\max_{\boldsymbol{\theta}} \Lambda(\boldsymbol{\theta}). \quad (3)$$

If $v(n)$ is non-Gaussian, the estimator $\hat{\boldsymbol{\theta}}$ in (3) coincides with the nonlinear least-squares solution. Maximizing $\Lambda(\boldsymbol{\theta})$ requires nonlinear programming, and with the objective function being nonconvex w.r.t. the unknowns, iterative gradient schemes may converge to local optima—a situation that becomes more likely when the parameter space to be searched is large. Motivated by the limitations of the ML solution, we pursue here a suboptimal approach to replace the multidimensional function maximization by successive one-dimensional (1-D) maximizations. If we are willing to trade off more computations for optimality, the suboptimal solutions can be used to initialize the ML algorithm in order to speed up the search required by (3) and prevent convergence to local minima.

The tool used in this work is a nonlinear transformation of the data that was originally introduced for continuous-time signals in [1] and was defined recursively as

$$\begin{aligned} s_1(n) &= s(n), \quad s_2(n;\tau_1) = s_1(n+\tau_1)s_1^*(n-\tau_1)\cdots \\ &\quad s_M(n;\tau_1,\tau_2,\cdots,\tau_{M-1}) \\ &= s_{M-1}(n+\tau_{M-1};\tau_1,\cdots,\tau_{M-2}) \\ &\quad \times s_{M-1}^*(n-\tau_{M-1};\tau_1,\cdots,\tau_{M-2}). \end{aligned} \quad (4)$$

We term s_M the multilag HIM (ml-HIM) because it reduces to the HIM for $\tau_1 = \cdots = \tau_{M-1} = \tau$, [19, ch. 12], [26]. Accordingly, we term the (generalized) Fourier series

$$\begin{aligned} &S_M(\alpha;\tau_1,\cdots,\tau_{M-1}) \\ &\quad := \lim_{N\to\infty}\frac{1}{N}\sum_{n=0}^{N-1} s_M(n;\tau_1,\cdots,\tau_{M-1})e^{-j\alpha n} \end{aligned} \quad (5)$$

multilag HAF (ml-HAF) because it generalizes to what Porat called high-order ambiguity function (HAF), [19, ch. 12], which corresponds to $S_M(\alpha;\tau,\cdots,\tau)$.

A. HIM and HAF of FM-PPS Signals

The HIM and the HAF were originally devised to estimate the phase coefficients $\{a_i\}$ of a PPS $\exp[j\phi_{\rm PPS}(n)]$ (see e.g., [18], [19, p. 393]). In the following, we show how they can be used to handle also sinusoidal or hyperbolic FM components. Applying the ml-HIM in (4) to the noise-free FM-PPS $s_1(n) = \rho\exp[j\phi_{\rm FM}(n)]\exp[j2\pi\sum_{i_0=0}^{M} a_{i_0}\ n^{i_0}/i_0!]$,

[1] For the hyperbolic FM, we assumed that the data are given by $\{x(n)\}_{n=1}^{N}$ to avoid $\ln(0)$.

we find

$$\begin{aligned} s_2(n;\tau_1) &= s_1(n+\tau_1)s_1^*(n-\tau_1) \\ &= \rho^2 s_2^{\mathrm{FM}}(n;\tau_1)\exp\left(j2\pi\sum_{i_0=0}^{M}(a_{i_0}/i_0!)\right. \\ &\quad \left.\times[(n+\tau_1)^{i_0}-(n-\tau_1)^{i_0}]\right) \\ &= \rho^2 s_2^{\mathrm{FM}}(n;\tau_1)\exp\left(j2\pi\sum_{i_0=0}^{M}(a_{i_0}/i_0!)\sum_{i_1=0}^{i_0}\right. \\ &\quad \left.\times\binom{i_0}{i_1}\tau_1^{i_0-i_1}n^{i_1}[1-(-1)^{i_0-i_1}]\right) \end{aligned} \tag{6}$$

where for the last equality, we used the binomial expansion. Signal $s_2^{\mathrm{FM}}(n;\tau_1)$ denotes the second-order HIM of $s^{\mathrm{FM}}(n) := \exp[j\phi_{\mathrm{FM}}(n)]$. If $i_0 = i_1 = M$ in (6), then $1-(-1)^{i_0-i_1} = 0$, and thus, $s_2(n;\tau_1)$ has a polynomial phase (in n) of order at most $M-1$. Repeating the differentiation and binomial expansion steps, the exponent can be made linear in n [cf. (4)]

$$\begin{aligned} &s_M(n;\boldsymbol{\tau}) \\ &= \rho^{2^{M-1}} s_M^{\mathrm{FM}}(n;\boldsymbol{\tau})\exp\left\{j2\pi\sum_{0\le i_{M-1}\le\cdots\le i_0\le M}\right. \\ &\quad\times\left[i_{M-1}!\prod_{m=1}^{M-1}(i_{m-1}-i_m)!\right]^{-1}a_{i_0} \\ &\quad\left.\times\prod_{m=1}^{M-1}[1-(-1)^{i_{m-1}-i_m}]\left(\prod_{m=1}^{M-1}\tau_m^{i_{m-1}-i_m}\right)n^{i_{M-1}}\right\} \end{aligned} \tag{7}$$

where we defined $\boldsymbol{\tau} := [\tau_1\tau_2\cdots\tau_{M-1}]$. Nonzero exponents appear in the PPS part of (7) only if $1-(-1)^{i_{m-1}-i_m} \neq 0$, $\forall\, m = 1, 2, \cdots, M-1$, which requires $0 < i_{M-2} < \cdots < i_1 < i_0$. If $i_0 = M-1$, then $i_1 = M-2, \cdots, i_{M-2} = 1$, $i_{M-1} = 0$, and the exponent in (7) includes the term $a_{M-1}\prod_{m=1}^{M-1}\tau_m\, n^0$. The linear (in n) term $a_M\prod_{m=1}^{M-1}\tau_m\, n^1$ also appears when $i_0 = M$. Hence, (7) reduces to

$$\begin{aligned} s_M(n;\boldsymbol{\tau}) &= \rho^{2^{M-1}} s_M^{\mathrm{FM}}(n;\boldsymbol{\tau}) \\ &\quad\times\exp\left(j2^M\pi(a_{M-1}+a_M n)\prod_{m=1}^{M-1}\tau_m\right). \end{aligned} \tag{8}$$

Correspondingly, the ml-HAF of (8) is given by [cf., (5)]

$$\begin{aligned} S_M(\alpha;\boldsymbol{\tau}) &= \rho^{2^{M-1}} S_M^{\mathrm{FM}}\left(\alpha - 2^M\pi a_M\prod_{m=1}^{M-1}\tau_m;\boldsymbol{\tau}\right) \\ &\quad\times\exp\left(j2^M\pi a_{M-1}\prod_{m=1}^{M-1}\tau_m\right). \end{aligned} \tag{9}$$

In the following, we specialize (8) and (9) to the cases of sinusoidal and hyperbolic FM.

B. Sinusoidal FM

In this case, we have $\phi_{\mathrm{FM}}(n) = 2\pi b\sin(\omega_0 n+\phi_0)$. With $M = 2$ (chirp), the second-order ml-HIM of (8) reduces to

$$\begin{aligned} s_2(n;\tau_1) &= \rho^2 s^{\mathrm{FM}}(n+\tau_1)s^{FM*}(n-\tau_1)e^{j4\pi\tau_1(a_1+a_2 n)} \\ &= \rho^2 e^{j4\pi b\,\sin(\omega_0\tau_1)\cos(\omega_0 n+\phi_0)}e^{j4\pi\tau_1(a_1+a_2 n)}. \end{aligned}$$

We observe that except for the $2\sin(\omega_0\tau_1)$ scale, the s_2^{FM} is also an FM signal. Similarly, using elementary trigonometric identities, the general Mth order ml-HIM is given by

$$\begin{aligned} s_M(n;\boldsymbol{\tau}) &= \rho^{2^{M-1}}\exp\left(j2^M\pi b\prod_{m=1}^{M-1}\right. \\ &\quad\left.\times\sin(\omega_0\tau_m)\sin[\omega_0 n+\phi_0+(M-1)\pi/2]\right) \\ &\quad\times\exp\left(j2^M\pi(a_{M-1}+a_M n)\prod_{m=1}^{M-1}\tau_m\right). \end{aligned} \tag{10}$$

Now, let us define

$$\omega_c := 2^M\pi a_M\prod_{m=1}^{M-1}\tau_m, \quad \psi_c := 2^M\pi a_{M-1}\prod_{m=1}^{M-1}\tau_m \tag{11}$$

$$\beta := 2^M\pi b\prod_{m=1}^{M-1}\sin(\omega_0\tau_m), \quad \psi_0 := \phi_0+(M-1)\pi/2 \tag{12}$$

where, for notational simplicity, we did not explicitly show the dependence of ω_c, ψ_c, and β on $\boldsymbol{\tau}$. Relying on (11) and (12), we can now put (10) in the equivalent form

$$s_M(n;\boldsymbol{\tau}) = \rho^{2^{M-1}}e^{j[\omega_c n+\psi_c+\beta\,\sin(\omega_0 n+\psi_0)]}. \tag{13}$$

Equation (13) shows that the Mth-order ml-HIM of a sinusoidal FM signal is still a sinusoidal FM signal, with the same vibration frequency ω_0 but with different modulation index β that is proportional to the original one b. Generally speaking, sinusoidal FM signals are "eigenfunctions" of the ml-HIM operator.

Being (almost) periodic,[2] in n, $s_M(n;\boldsymbol{\tau})$ of (13) can be written as a superposition of equally spaced harmonics $\{\omega_c \pm k\omega_0\}$ with amplitudes $\{J_k(\beta)\}$, which are the kth-order Bessel functions of the first kind, [24, p. 311].

$$s_M(n;\boldsymbol{\tau}) = \rho^{2^{M-1}}\sum_{k=-\infty}^{\infty}J_k(\beta)e^{j[(\omega_c+k\omega_0)n+\psi_c+k\psi_0]}. \tag{14}$$

Closed-form expressions are not available for $J_k(\beta)$, but the following relations are known to hold (see e.g., [24, p. 311]):

$$J_{-k}(\beta) = (-1)^k J_k(\beta), \quad \sum_{k=-\infty}^{\infty}J_k^2(\beta) = 1 \tag{15}$$

$$e^{(\beta/2)(s-(1/s))} = \sum_{k=-\infty}^{\infty}J_k(\beta)\,s^k, \quad 0 < |s| < \infty. \tag{16}$$

[2]Signal $s_M(n;\boldsymbol{\tau})$ would be strictly periodic only if $\{T_k := 2\pi/(\omega_c \pm k\omega_0)\}$ were integers $\forall\, k$; see [9] for rigorous definitions of almost periodic functions.

Because $J_k(\beta)$ vanishes for large $|k|$ [24], there exists a large enough integer K such that most of the energy in $\{J_k(\beta)\}$ is contained in the range $k \in [-K, K]$. It has been shown in [27] that the smallest integer K for which $\sum_{k=-K}^{K} J_k^2(\beta) > 0.99$ is $K \approx \beta + 1$ for $\beta > 1$, whereas $K = 0$ for $\beta \in [0, 0.14)$. For $\beta \in [0.14, 1]$, K is either 1 or 2. Depending on β, we can thus approximate the infinite sum in (14) by the partial sum

$$s_M(n; \boldsymbol{\tau}) = \rho^{2^{M-1}} \sum_{k=-K}^{K} J_k(\beta) e^{j[(\omega_c + k\omega_0)n + \psi_c + k\psi_0]} \quad (17)$$

which consists of multicomponent constant amplitude tones with harmonic frequencies. Fourier transforming (17), we obtain the ml-HAF as

$$S_M(\alpha; \boldsymbol{\tau}) = \rho^{2^{M-1}} \sum_{k=-K}^{K} J_k(\beta) e^{j(\psi_c + k\psi_0)} \delta(\alpha - \omega_c - k\omega_0) \quad (18)$$

where $\delta(\cdot)$ denotes the Kronecker delta function

$$\delta(\alpha) := \begin{cases} 1, & \alpha = 0 \bmod (2\pi) \\ 0, & \text{otherwise.} \end{cases} \quad (19)$$

The ml-HAF in (18) peaks at $\{\omega_c + k\omega_0\}_{k=-K}^{K}$. Hence, the vibration frequency ω_0 is given by the distance between successive peaks of $|S_M(\alpha; \boldsymbol{\tau})|$. The position of the central peak is related to the highest order PPS coefficient a_M through ω_c [cf. (11)]. Then, making use of (16), we can obtain β and ψ_0 and, subsequently, the modulation index b and the phase ϕ_0 from the values at the peaks. In Section III, we will detail how to use these relationships to estimate the parameters of interest. For the moment, let us focus on narrowband sinusoidal FM signals.

C. Narrowband Sinusoidal FM

According to Carson's rule, the bandwidth of an FM signal is approximately $2\omega_0(1 + \beta)$ [24, p. 313]. We will refer to the case discussed so far, for general β, as the wideband FM (WBFM). Expanding $\exp[j\beta \sin(\omega_0 n + \psi_0)]$ in Taylor series, we find

$$e^{j\beta \sin(\omega_0 n + \psi_0)} = \sum_{k=0}^{\infty} \frac{[j\beta \sin(\omega_0 n + \psi_0)]^k}{k!}. \quad (20)$$

If β is small enough, we can truncate the series expansion as

$$\begin{aligned} e^{j\beta \sin(\omega_0 n + \psi_0)} &= \sum_{k=0}^{\infty} \frac{[j\beta \sin(\omega_0 n + \psi_0)]^k}{k!} \\ &\approx 1 + j\beta \sin(\omega_0 n + \psi_0) \\ &\quad - \tfrac{1}{2}\beta^2 \sin^2(\omega_0 n + \psi_0) \\ &= 1 - \frac{\beta^2}{4} + j\beta \sin(\omega_0 n + \psi_0) \\ &\quad + \frac{\beta^2}{4} \cos(2\omega_0 n + 2\psi_0). \end{aligned} \quad (21)$$

A value of $\beta < 1$ is sufficient to guarantee that the second-order approximation is sufficiently accurate. We will refer to the case of $\beta < 1$ as narrowband FM (NBFM). Using (21) in (13), we obtain

$$\begin{aligned} S_M(\alpha; \boldsymbol{\tau}) \approx \rho^{2^{M-1}} \Bigg[& \frac{\beta^2}{8} e^{j(\psi_c - 2\psi_0)} \delta(\alpha - \omega_c + 2\omega_0) \\ & + \frac{\beta}{2} e^{j(\psi_c - \psi_0)} \delta(\alpha - \omega_c + \omega_0) + \left(1 - \frac{\beta^2}{4}\right) \\ & \times e^{j\psi_c} \delta(\alpha - \omega_c) + \frac{\beta}{2} e^{j(\psi_c + \psi_0)} \delta(\alpha - \omega_c - \omega_0) \\ & + \frac{\beta^2}{8} e^{j(\psi_c + 2\psi_0)} \delta(\alpha - \omega_c - 2\omega_0) \Bigg] \end{aligned} \quad (22)$$

which makes estimation of β from the amplitude of the peaks easier, as it will be shown in the next section. Note that the bandwidth of the signal in (22) is $4\omega_0$, as predicted by Carson's rule (with $\beta = 1$). It is worth observing that because $\beta = 2^M \pi b \prod_{m=1}^{M-1} \sin(\omega_0 \tau_m)$, it is possible to select the lags $\boldsymbol{\tau}$ in order to have $\beta < 1$. Because ω_0 is unknown, we use the estimate ω_0 to select the set of lags in such a way that $\beta < 1$. This allows estimation of β using the second-order approximation (22).

D. Hyperbolic FM

In this case, we have $\phi_{\mathrm{FM}}(n) = 2\pi\gamma \ln(n)$. From (4), the second-order ml-HIM of the FM part is

$$\begin{aligned} s_2^{\mathrm{FM}}(n; \tau_1) &= e^{j2\pi\gamma \ln(n+\tau_1)} e^{-j2\pi\gamma \ln(n-\tau_1)} \\ &= e^{j2\pi\gamma \ln[(n+\tau_1)/(n-\tau_1)]} \end{aligned} \quad (23)$$

and the third-order ml-HIM is given by

$$\begin{aligned} & s_3^{\mathrm{FM}}(n; \tau_1, \tau_2) \\ & \quad = \exp\left(j2\pi\gamma \ln\left[\frac{(n + \tau_2 + \tau_1)(n - \tau_2 - \tau_1)}{(n + \tau_2 - \tau_1)(n - \tau_2 + \tau_1)} \right] \right). \end{aligned} \quad (24)$$

The general Mth-order ml-HIM of the FM component can be written as

$$s_M^{\mathrm{FM}}(n; \boldsymbol{\tau}) = e^{j2\pi\gamma \ln[g_M(n; \boldsymbol{\tau})]} \quad (25)$$

where we defined

$$g_M(n; \boldsymbol{\tau}) := \frac{\prod_{\substack{k=1 \\ \mathbf{i}_k \in S_E}}^{2^{M-2}} \left(n + \sum_{m=1}^{M-1} (-1)^{i_{m,k}} \tau_m \right)}{\prod_{\substack{k=1 \\ \mathbf{i}_k \in S_O}}^{2^{M-2}} \left(n + \sum_{m=1}^{M-1} (-1)^{i_{m,k}} \tau_m \right)} \quad (26)$$

and S_E, S_O are two sets containing 2^{M-2} different elements, each element $\mathbf{i}_k$ being a sequence of zeros and ones, i.e., $\mathbf{i}_k := [i_{1,k}\ i_{2,k}\ \cdots\ i_{M-1,k}]$ with $i_{i,k} \in \{0, 1\}$. The vector $\mathbf{i}_k \in S_E$ if and only if $\sum_{j=1}^{M-1} i_{j,k}$ is an even number and $\mathbf{i}_k \in S_O$ otherwise. In other words, $\mathbf{i}_k \in S_E$ iff it contains an even number of ones, whereas $\mathbf{i}_k \in S_O$ iff it contains an odd number of ones. Inserting (25) in (8), we find the Mth-order ml-HIM for the hybrid PPS-hyperbolic FM signal as

$$\begin{aligned} s_M(n; \boldsymbol{\tau}) = \rho^{2^{M-1}} & \exp\left(j2^M \pi \prod_{m=1}^{M-1} \tau_m (a_{M-1} + a_M n) \right) \\ & \times e^{j2\pi\gamma \ln[g_M(n; \boldsymbol{\tau})]}. \end{aligned} \quad (27)$$

Similarly, we derive the $(M+1)$st order ml-HIM as

$$s_{M+1}(n;\boldsymbol{\tau}) = \rho^{2^M} \exp\left(j2^{M+1}\pi a_M \prod_{m=1}^{M} \tau_m\right) \times e^{j2\pi\gamma \ln[g_{M+1}(n;\boldsymbol{\tau})]}. \quad (28)$$

Note that $\boldsymbol{\tau}$ denotes the $(M-1)$-dimensional vector $[\tau_1 \ \tau_2 \ \cdots \ \tau_{M-1}]$ in (25), and the M-dimensional vector $[\tau_1 \ \cdots \ \tau_{M-1} \ \tau_M]$ in (28). In contrast to sinusoidal FM, hyperbolic FM signals are not "eigenfunctions" of the ml-HIM operator. In the next section, it will be shown how to use (27) and (28) to estimate γ and $\{a_i\}_{i=0}^{M}$.

III. Parameter Estimation

In the previous sections, we have derived relationships between the parameters of interest and the ml-HAF of the noise-free signal $s(n)$. In a realistic scenario, the desired signal is contaminated by additive noise, and we observe

$$x(n) = \rho e^{j\phi_{\mathrm{FM}}(n)} e^{j\phi_{\mathrm{PPS}}(n)} + v(n), \quad n = 0, 1, \cdots, N-1. \quad (29)$$

We assume that $v(n)$ is zero-mean complex white Gaussian, stationary and mixing in the sense of [8, p. 25] with variance σ_v^2. Sample estimates of $s_M(n;\boldsymbol{\tau})$ and $S_M(\alpha;\boldsymbol{\tau})$ in (8) and (9) are computed from $\{x(n)\}_{n=0}^{N-1}$, respectively, as

$$\hat{s}_M(n;\boldsymbol{\tau}) = x_M(n;\boldsymbol{\tau}) \quad (30)$$

$$\hat{S}_M(\alpha;\boldsymbol{\tau}) = \frac{1}{N}\sum_{n=0}^{N-1} \hat{s}_M(n;\boldsymbol{\tau})\, e^{-j\alpha n} = \frac{1}{N}\sum_{n=0}^{N-1} x_M(n;\boldsymbol{\tau})\, e^{-j\alpha n} \quad (31)$$

where $x_M(n;\boldsymbol{\tau})$ is the ml-HIM, and $\hat{S}_M(\alpha;\boldsymbol{\tau}) = X_M(\alpha;\boldsymbol{\tau})$ is the ml-HAF of the data $x(n)$. Under the stated assumptions on $v(n)$, estimators in (30) and (31) are asymptotically unbiased and consistent in the mean square sense (see [26] for proof), e.g., for the estimator in (31), we have

$$\lim_{N\to\infty} E\{\hat{S}_M(\alpha;\boldsymbol{\tau})\} = \lim_{N\to\infty} E\{X_M(\alpha;\boldsymbol{\tau})\} = S_M(\alpha;\boldsymbol{\tau})$$
$$\lim_{N\to\infty} \mathrm{var}\{\hat{S}_M(\alpha;\boldsymbol{\tau})\} = 0. \quad (32)$$

Once $\hat{S}_M(\alpha;\boldsymbol{\tau})$ is computed, $\boldsymbol{\theta}_{\mathrm{PPS}}$ and $\boldsymbol{\theta}_{\mathrm{FM}}$ can be estimated by substituting $\hat{S}_M(\alpha;\boldsymbol{\tau})$ for $S_M(\alpha;\boldsymbol{\tau})$ in the relationships derived in the previous section.

A. Sinusoidal FM Parameter Estimation

Equation (18) shows that the peaks occur in the HAF at $\{\omega_c + k\omega_0\}_{k=-K}^{K}$, with $\omega_c = 2^M\pi a_M \prod_{m=1}^{M-1}\tau_m$. Note that ω_c depends on the lags only through their product. Thus, we can take advantage of the multiple lags and calculate X_M for L different sets of lags, $\boldsymbol{\tau_l} := [\tau_{1,l} \cdots \tau_{M-1,l}]$, $l = 1, 2, \cdots, L$, having the same product, i.e., $\prod_{m=1}^{M-1}\tau_{m,l_1} = \prod_{m=1}^{M-1}\tau_{m,l_2}$, $\forall l_1, l_2 \in [1, L]$. The product of L ml-HAF amplitudes $\prod_{l=1}^{L}|X_M(\alpha,\boldsymbol{\tau_l})|$ enhances the desired peaks and reduces noise further than the single ml-HAF [2]. From (12), different sets of lags imply different values of β and produce different estimates of b, whose averaging may improve accuracy. With known ρ, the resulting algorithm is summarized in the following steps (estimation of ρ is addressed in the following subsection):

Step 1) Calculate from the data $x_M(n;\boldsymbol{\tau_l})$ the ml-HIM of order M for each set of lags $\boldsymbol{\tau_l}$, $l = 1, 2, \cdots, L$.

Step 2) Estimate the ml-HAF of $s(n)$ using (31).

Step 3) Find the peak location of the product ml-HAF, $\prod_{l=1}^{L}|\hat{S}_M(\alpha,\boldsymbol{\tau_l})| = \prod_{l=1}^{L}|X_M(\alpha,\boldsymbol{\tau_l})|$ corresponding to $\{\omega_c + k\omega_0\}_{k=-K}^{K}$ [see also (18)], and collect these values in a $(2K+1)\times 1$ vector $\hat{\boldsymbol{p}}$.

Step 4) Define

$$\mathbf{k} := [-K \ -K+1 \ \cdots \ K-1 \ K]^T \quad (33)$$
$$\mathbf{1} := [1\ 1\ \cdots\ 1]^T, \quad \mathbf{A} := [\mathbf{k}\ \mathbf{1}], \quad \hat{\omega} := [\hat{\omega}_0\, \hat{\omega}_c]^T. \quad (34)$$

Solve the overdetermined linear system $\mathbf{A}\hat{\omega} \overset{LS}{=} \hat{\mathbf{p}}$ to compute $\hat{\omega}_0$ and $\hat{\omega}_c$ as

$$\hat{\omega} = \begin{bmatrix}\hat{\omega}_0 \\ \hat{\omega}_c\end{bmatrix} = (\mathbf{A}^T\mathbf{A})^{-1}\mathbf{A}^T\hat{\mathbf{p}}. \quad (35)$$

Step 5) Estimate a_M as

$$\hat{a}_M = \frac{\hat{\omega}_c}{2^M\pi \prod_{m=1}^{M-1}\tau_{m,1}}. \quad (36)$$

Step 6) Estimating b from (18) and (12) requires some care because (18) is exact only as $N\to\infty$. For finite sample size, we find from (31) that

$$\hat{S}_M(\omega_c + k\omega_0;\boldsymbol{\tau_l}) = \text{noise terms} + \rho^{2^{M-1}} \frac{N - 2\sum_{m=1}^{M-1}\tau_{m,l}}{N} J_k(\beta_l) e^{j(\psi_c + k\psi_0)} \quad (37)$$

where $\beta_l := 2^M\pi b \prod_{m=1}^{M-1}\sin(\omega_0\tau_{m,l})$. To estimate b based on (37), we first find

$$\hat{J}_k(\beta_l) = \frac{\hat{S}_M(\hat{\omega}_c + k\hat{\omega}_0;\boldsymbol{\tau_l})}{\rho^{2^{M-1}}\left(N - 2\sum_{m=1}^{M-1}\tau_{m,l}\right)\Big/N} \quad \text{for } k\in[-K, K]. \quad (38)$$

We then use (16) to estimate β_l as (see also [27])

$$\hat{\beta}_l = \frac{2s}{s^2-1}\ln\left[\sum_{k=-K}^{K}\hat{J}_k(\beta_l)\, s^k\right] \quad (39)$$

or, from the standard deviation of the power spectrum, as suggested in [12]

$$\hat{\beta}_l = \sqrt{\frac{2\sum_{k=-K}^{K} k^2\hat{J}_k^2(\beta_l)}{\sum_{k=-K}^{K}\hat{J}_k^2(\beta_l)}}. \quad (40)$$

Finally, obtain an estimate of b via (12) as

$$\hat{b} = \frac{1}{L}\sum_{l=1}^{L} \frac{\hat{\beta}_l}{2^M \pi \prod_{m=1}^{M-1} \sin(\hat{\omega}_0 \tau_{m,l})}. \quad (41)$$

Note from (12) that when $\prod_{m=1}^{M-1} \sin(\hat{\omega}_0 \tau_{m,l}) < 0$, then $\beta_l < 0$, and in this case, (40) furnishes only an estimate of $|\beta_l|$. However, this is not a problem because by definition $b > 0$, and hence, $\hat{b}$ is obtained as the ratio of the two absolute values.

Step 7) With arg denoting (unwrapped) phase, define

$$\hat{\boldsymbol{\Psi}} := [\hat{\boldsymbol{\Psi}}_0 \ \hat{\boldsymbol{\Psi}}_c]^T, \quad \hat{\Psi}_{k,l} := \arg\{\hat{S}_M(\hat{\omega}_c + k\hat{\omega}_0; \boldsymbol{\tau}_l)\} \quad (42)$$

$$\hat{\boldsymbol{\Psi}}_l := [\hat{\Psi}_{-K,l} \ \cdots \ \hat{\Psi}_{K,l}]^T, \quad \hat{\boldsymbol{\Psi}} := [\hat{\boldsymbol{\Psi}}_1^T \ \cdots \ \hat{\boldsymbol{\Psi}}_L^T]^T \quad (43)$$

and the $(2M+1)L \times 2$ dimensional matrix $\mathbf{B}$ as

$$\mathbf{B} := [\underbrace{\mathbf{A}^T \ \mathbf{A}^T \ \cdots \ \mathbf{A}^T}_{L}]^T. \quad (44)$$

Solve the overdetermined linear system $\mathbf{B}\hat{\boldsymbol{\Psi}} \overset{LS}{=} \hat{\boldsymbol{\Psi}}$ to find $\hat{\boldsymbol{\Psi}}_0$ and $\hat{\boldsymbol{\Psi}}_c$

$$\hat{\boldsymbol{\Psi}} = \begin{bmatrix} \hat{\boldsymbol{\Psi}}_0 \\ \hat{\boldsymbol{\Psi}}_c \end{bmatrix} = (\mathbf{B}^T\mathbf{B})^{-1}\mathbf{B}^T\hat{\boldsymbol{\Psi}}. \quad (45)$$

Then, $\hat{\boldsymbol{\psi}}_0$ is obtained as $\hat{\phi}_0 = \hat{\psi}_0 - (M-1)\pi/2$. Now, having estimated a_M and the FM component, we can remove it from the data and proceed with the PPS part using techniques described in [26]. For example, if $M = 3$ we proceed to the next step.

Step 8) Remove the estimated terms from the data by demodulation

$$x_1(n) := x(n)\, e^{-j2\pi[\hat{a}_3 n^3/6 + \hat{b}\ \sin(\hat{\omega}_0 n + \hat{\phi}_0)]}. \quad (46)$$

The second-order ml-HAF of $x_1(n)$ peaks at $\alpha_l = 4\pi\tau_{1,l}a_2$; therefore, we estimate a_2 as

$$\hat{a}_2 = \frac{1}{L}\sum_{l=1}^{L} \frac{\hat{\alpha}_l}{4\pi\tau_{1,l}}. \quad (47)$$

Note that a_{M-1} (a_2 in this case) can also be estimated from $\hat{\psi}_c$.

Step 9) Estimate a_1 by removing $\hat{a}_2$:

$$x_2(n) := x_1(n)\, e^{-j2\pi\hat{a}_2 n^2/2} \quad (48)$$

whose DFT $X_2(\alpha)$ peaks at $2\pi a_1$. Finally, a_0 can be estimated from the phase of $X_2(2\pi\hat{a}_1)$ or via linear least squares [26].

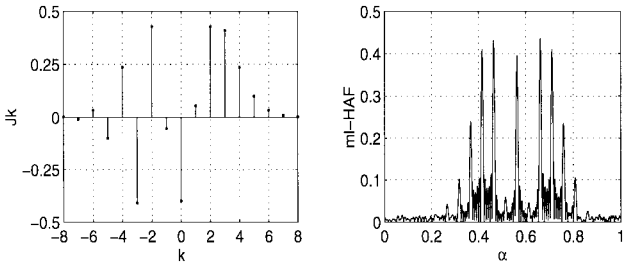

Fig. 1. (a) Bessel coefficients $J_k(\beta)$ versus k for $\beta = 3.6996$ and (b) $X_2(\alpha;\, \tau_1)$ versus α for SNR = 16 dB and $N = 1024$.

As an example, in Fig. 1(a), we plot the values of the Bessel coefficients $J_k(\beta)$ versus k for $b = 6$, $\omega_0 = 0.0491$, $\tau_1 = 129$. From (11) and (12), we find $\omega_c = 0.5629$ and $\beta = 3.6996$. The values of the other parameters can be found in Example 2 in Section IV. As expected, the coefficients become negligible for $|K| > 5$ in (17), confirming that $K \approx \beta + 1$. In Fig. 1(b), the ml-HAF $X_2(\alpha; \tau_1)$ is plotted for $\alpha \in [0, 1]$, SNR $:= \rho^2/\sigma_v^2 = 16$ dB, and $N = 1024$. From the location (and value) of the peaks, we derive our estimates. A couple of remarks are now in order.

Remark 1: In recovering the FM parameters two issues arise: i) identifiability and ii) estimation accuracy. If we use lags causing $\sin(\omega_0\tau_m) = 0$, then β in (12) vanishes, and the modulation index b in (41) is nonidentifiable. However, this problem is not only discernible (from the presence of a single peak in the HAF) but also fixable when we consider appropriately chosen lags in the HAF. Specifically, suppose that we start with a set of lags $\boldsymbol{\tau}_0 := (\tau_0, \cdots, \tau_0)$ and observe a single peak in the HAF. This is impossible if $\tau_0 = 1$ because by our modeling assumption, the FM component is present, and hence, $\omega_0 \neq 0, \pi$. If, on the other hand, $\tau_0 = \tau > 1$ and a single peak emerges in the HAF, we infer two things: First, that $\omega_0 = \pi/\tau$, and second, that by using $\tau_0 \neq \tau$, identifiability of the modulation component can be established in at most two steps.

Remark 2: In Step 3 of our algorithm, the number of peaks $(2K+1)$ varies as a function of the modulation index β. Indeed, when using $\{\boldsymbol{\tau}_l\}_{l=0}^{L-1}$ sets of lags in the product ml-HAF, we may loose some peaks and end up with $2K+1$ peaks, where now, $K := \min_{l\in[0,L-1]} K_l$, and K_l denotes the lag-dependent number of peaks arising in the ml-HAF that uses the set $\boldsymbol{\tau}_l$. From an estimation point of view, more peaks may help due to averaging in the least-squares approach of Step 3, but fundamentally, their number does not influence identifiability as long as $K \geq 1$. Hence, Step 3 and our FM parameters have no identifiability problems in our algorithm. In our simulations, we fixed K by inspecting the dominant peaks in the product ml-HAF. Estimate of the peaks' locations can be made completely automatic by using the prediction error filter (PEF) approach of [23]; this alternative procedure is not investigated here (see [23] for more details).

Narrowband FM: When $\beta < 1$, we use (22) to modify step 6 as follows.

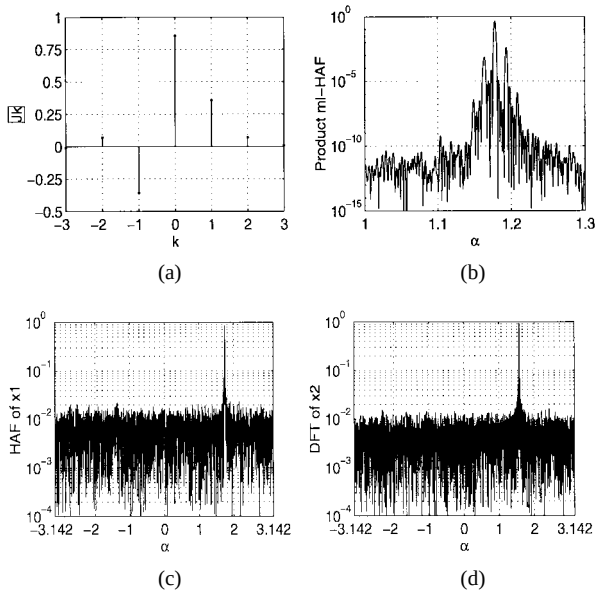

Fig. 2. (a) Bessel coefficients $J_k(\beta)$ versus k for $\beta = 0.7711$ and (b)–(d) plots for estimating the FM-PPS parameters.

Step 6 (NBFM): Exploit (22) to obtain different estimates of β as

$$\hat{\beta}_{0,l} = 2\sqrt{1 - \frac{|\hat{S}_M(\hat{\omega}_c; \boldsymbol{\tau}_l)|}{\rho^{2^{M-1}}\left(N - 2\sum_{m=1}^{M-1}\tau_{m,l}\right)\Big/N}}$$

$$\hat{\beta}_{1,l} = \frac{|\hat{S}_M(\hat{\omega}_c + \hat{\omega}_0; \boldsymbol{\tau}_l)| + |\hat{S}_M(\hat{\omega}_c - \hat{\omega}_0; \boldsymbol{\tau}_l)|}{\rho^{2^{M-1}}\left(N - 2\sum_{m=1}^{M-1}\tau_{m,l}\right)\Big/N}$$

$$\hat{\beta}_{2,l} = 2\sqrt{\frac{|\hat{S}_M(\hat{\omega}_c + 2\hat{\omega}_0; \boldsymbol{\tau}_l)| + |\hat{S}_M(\hat{\omega}_c - 2\hat{\omega}_0; \boldsymbol{\tau}_l)|}{\rho^{2^{M-1}}\left(N - 2\sum_{m=1}^{M-1}\tau_{m,l}\right)\Big/N}} \quad (49)$$

and then take their mean $\hat{\beta} = (1/3L)\sum_{l=1}^{L}\sum_{i=0}^{2}\hat{\beta}_{i,l}$. Finally, $\hat{b}$ is derived by inserting $\hat{\beta}$ in (41). The other steps remain unchanged.

In Fig. 2(a), we plot the values of the Bessel coefficients $J_k(\beta)$ versus k for $b = 0.05$, $\omega_0 = 0.015$, and $\tau_{1,1} = \tau_{2,1} = 60$ so that $\beta = \beta_1 = 0.7711$ (the values of the other parameters are reported in Example 1). As expected, when $\beta < 1$, we can approximate the infinite sum in (14) by the partial sum with $K = 2$. In Fig. 2(b), the product ml-HAF $\prod_{l=1}^{6}|X_3(\alpha, \boldsymbol{\tau}_l)|$ is plotted in $\alpha \in [1, 1.3]$ for SNR $= 12$ dB, and $N = 2048$. The five peaks relative to $\{\omega_c + k\omega_0\}_{k=-2}^{2}$ are recognizable. In Fig. 2(c) and (d), the second-order HAF of $x_1(n)$ in (46) and the DFT of $x_2(n)$ in (48) are plotted for $\alpha \in [-\pi, \pi]$. They show sharp peaks, whose locations furnish the estimates of a_2 and a_1, respectively.

B. Estimation of ρ and σ_v^2

Thus far, we have considered the amplitude ρ to be known. If ρ is unknown, we cannot use the approach proposed in [26], where $\rho\exp(j2\pi a_0)$ is estimated via linear least squares since knowledge of ρ is necessary in Step 6. In [27], an algorithm for the joint estimation of ρ and β was suggested; here, we propose an alternative approach based on second- and fourth-order statistics that has the advantage of separating estimation of ρ and σ_v^2 from the PPS and FM parameters (as it will be shown in the next section, the relevant Cramér–Rao bounds are also decoupled). With $x(n)$ as in (29), our method is based on the following observation:

$$E\{|x(n)|^2\} = \rho^2 + \sigma_v^2, \quad E\{|x(n)|^4\} = \rho^4 + 4\rho^2\sigma_v^2 + \sigma_v^4. \quad (50)$$

Therefore

$$\rho^4 = 2E^2\{|x(n)|^2\} - E\{|x(n)|^4\}, \quad \sigma_v^2 = E\{|x(n)|^2\} - \rho^2. \quad (51)$$

Thus, estimators for ρ and σ_v^2 are obtained by replacing ensemble quantities in (51) with sample single record estimates

$$\hat{\rho} = \left[2\left(\frac{1}{N}\sum_{n=0}^{N-1}|x(n)|^2\right)^2 - \frac{1}{N}\sum_{n=0}^{N-1}|x(n)|^4\right]^{1/4} \quad (52)$$

$$\hat{\sigma}_v^2 = \frac{1}{N}\sum_{n=0}^{N-1}|x(n)|^2 - \hat{\rho}^2. \quad (53)$$

Unbiasedness and mean square consistency follow from the mixing conditions assumed to be satisfied for $v(n)$; the proof is standard and is not reported here.

C. Hyperbolic FM Parameter Estimation

The problem of estimating γ and $\{a_i\}_{i=0}^{M}$ can be decoupled by using (28). The hyperbolic parameter can be estimated via a nonlinear least-square matching approach. Specifically, treating $\hat{s}_{M+1}(n; \boldsymbol{\tau}_l)$ as "data," we minimize with respect to γ the following statistic:

$$\begin{aligned} Q_N(\gamma, a_M) &:= \sum_{n=1}^{N}|\hat{s}_{M+1}(n; \boldsymbol{\tau}_l) - s_{M+1}(n; \boldsymbol{\tau}_l)|^2 \\ &= \sum_{n=1}^{N}\Bigg|\hat{s}_{M+1}(n; \boldsymbol{\tau}_l) - \rho^{2^M} \\ &\quad \times \exp\left(j2^{M+1}\pi a_M\prod_{m=1}^{M}\tau_m\right) \\ &\quad \times e^{j2\pi\gamma\ln[g_{M+1}(n;\boldsymbol{\tau})]}\Bigg|^2. \end{aligned} \quad (54)$$

Recalling (30), $\hat{s}_{M+1}(n; \boldsymbol{\tau}_l) = x_{M+1}(n; \boldsymbol{\tau}_l)$, and after straightforward manipulations, estimation of γ reduces to

$$\hat{\gamma} = \arg\max_{\gamma}\left|\sum_{n=1}^{N}x_{M+1}(n; \boldsymbol{\tau}_l)e^{-j2\pi\gamma\ln[g_{M+1}(n;\boldsymbol{\tau}_l)]}\right| \quad (55)$$

that can be solved by grid search. Alternatively, we can resort to a Newton–Raphson or a scoring approach (see [6] for a thorough description of nonlinear optimization methods applied to estimation problems). The accuracy can be improved

by using different sets of lags $\boldsymbol{\tau_l}$, averaging with respect to l, and then maximizing the result

$$\hat{\gamma} = \arg\max_{\gamma} \sum_{l=1}^{L} \left| \sum_{n=1}^{N} x_{M+1}(n;\boldsymbol{\tau_l}) e^{-j2\pi\gamma \ln[g_{M+1}(n;\boldsymbol{\tau_l})]} \right|. \tag{56}$$

It is worth noting that the quantity to be maximized does not depend on ρ; therefore, the same estimation algorithm can be applied when the amplitude is unknown.

Fig. 3(a) shows a realization of the (random) functional in (56) to be maximized, for $M = 2$, $\tau_1 = \tau_2 = 30$, SNR = 10 dB, $N = 256$, $\gamma = 5$, and the other parameters set as in Example 3. We can observe that the function to be maximized has a discernible peak so that the search for the maximum can be carried out easily. Once γ has been estimated, we can remove its contribution from the data and proceed with the PPS part using techniques already described for the sinusoidal FM case. After the hyperbolic term removal, we have the *new* (demodulated) data

$$\begin{aligned} y(n) &:= x(n) e^{-j2\pi\hat{\gamma} \ln(n)} \\ &= \rho \exp\left(j2\pi \sum_{i=0}^{M} a_i n^i \Big/ i! \right) e^{j2\pi\gamma_e \ln(n)} \\ &\quad + \text{noise terms} \end{aligned} \tag{57}$$

where we defined $\gamma_e := \gamma - \hat{\gamma}$. Therefore, the *new* data have the same structure of the original data but with γ replaced by γ_e (note that, in general, $\gamma_e \ll \gamma$). To understand the effect of γ_e, let us consider for a moment only the signal component of the data and call it $s(n)$. The Mth-order ml-HIM of $s(n)$ is given by [cf., (27)]

$$\begin{aligned} s_M(n;\boldsymbol{\tau_l}) = \rho^{2^{M-1}} &\exp\left(j2^M\pi \prod_{m=1}^{M-1} \tau_{m,l} \left(a_{M-1} + a_M\, n\right) \right) \\ &\times e^{j2\pi\gamma_e \ln[g_M(n;\boldsymbol{\tau_l})]}. \end{aligned} \tag{58}$$

The ml-HAF is obtained by taking the Fourier transform of (58)

$$\begin{aligned} S_M(\alpha;\boldsymbol{\tau_l}) = \rho^{2^{M-1}} &\exp\left(j2^M\pi a_{M-1} \prod_{m=1}^{M-1} \tau_m \right) \\ &\times S_M^{\mathrm{FM}}\left(\alpha - 2^M\pi a_M \prod_{m=1}^{M-1} \tau_{m,l};\, \boldsymbol{\tau_l} \right) \end{aligned} \tag{59}$$

where $S_M^{\mathrm{FM}}(\alpha;\boldsymbol{\tau_l})$ again denotes the Mth-order ml-HAF of the (hyperbolic) FM component. With finite samples, consistent estimates of $S_M(\alpha;\boldsymbol{\tau_l})$ are obtained as [cf., (31)]

$$\hat{S}_M(\alpha;\boldsymbol{\tau_l}) = \frac{1}{N} \sum_{n=0}^{N-1} y_M(n;\boldsymbol{\tau_l})\, e^{-j\alpha n} \tag{60}$$

where $y_M(n;\boldsymbol{\tau_l})$ is the ml-HIM of the *new* data $y(n)$. It is important now to understand what we obtain from the ml-HAF estimator in (60). The signal component is given by

$$\begin{aligned} \hat{S}_M(\alpha;\boldsymbol{\tau_l}) &= \frac{1}{N} \sum_{n=0}^{N-1} s_M(n;\boldsymbol{\tau_l})\, e^{-j\alpha n} \\ &= \rho^{2^{M-1}} \exp\left(j2^M\pi a_{M-1} \prod_{m=1}^{M-1} \tau_{m,l} \right) \\ &\quad \times \frac{1}{N} \sum_{n=0}^{N-1} e^{j2\pi\gamma_e \ln[g_M(n;\boldsymbol{\tau_l})]} \\ &\quad \times \exp\left(-j\left(\alpha - 2^M\pi a_M \prod_{m=1}^{M-1} \tau_{m,l} \right) n \right) \\ &= \rho^{2^{M-1}} \exp\left(j2^M\pi a_{M-1} \prod_{m=1}^{M-1} \tau_{m,l} \right) \hat{S}_M^{\mathrm{FM}} \\ &\quad \times \left(\alpha - 2^M\pi a_M \prod_{m=1}^{M-1} \tau_{m,l};\, \boldsymbol{\tau_l} \right). \end{aligned} \tag{61}$$

Unfortunately

$$\hat{S}_M^{\mathrm{FM}}(\alpha;\boldsymbol{\tau_l}) := N^{-1} \sum_{n=0}^{N-1} e^{j2\pi\gamma_e \ln[g_M(n;\boldsymbol{\tau_l})} e^{-j\alpha n}$$

is not known for finite N. However, for N large enough, we can obtain a useful closed-form relationship. In the Appendix, we prove that $\lim_{N\to\infty} \hat{S}_2^{\mathrm{FM}}(\alpha;\tau_1) = \delta(\alpha)$. This result is of interest because, coupled with (59), it allows us to infer that (see the Appendix for a proof)

$$\begin{aligned} \lim_{N\to\infty} \hat{S}_M(\alpha;\boldsymbol{\tau_l}) = \rho^{2^{M-1}} &\exp\left(j2^M\pi a_{M-1} \prod_{m=1}^{M-1} \tau_{m,l} \right) \\ &\delta\left(\alpha - 2^M\pi a_M \prod_{m=1}^{M-1} \tau_{m,l} \right). \end{aligned} \tag{62}$$

The Mth-order ml-HAF in (62) peaks at $\alpha = 2^M\pi a_M \prod_{m=1}^{M-1} \tau_{m,l}$; hence, we can estimate a_M from the peak location of $\hat{S}_M(\alpha;\boldsymbol{\tau_l})$ derived as in (60). Accuracy can then be improved by averaging the estimates obtained for different sets of lags

$$\hat{a}_M = \frac{1}{L} \sum_{l=1}^{L} \frac{1}{2^M\pi \prod_{m=1}^{M-1} \tau_{m,l}} \arg\max_{\alpha} |\hat{S}_M(\alpha;\boldsymbol{\tau_l})|. \tag{63}$$

In Fig. 3(b), a realization of $|\hat{S}_M(\alpha;\boldsymbol{\tau_l})| = |Y_M(\alpha;\boldsymbol{\tau_l})|$ is reported, for $M = 2$, $\tau_1 = \tau_2 = 30$, SNR = 10 dB, $N = 256$, $\gamma = 5$, $a_2 = 1.0208 \cdot 10^{-3}$; therefore, the plot should peak (approximately) at $\alpha = 0.0612$. Once a_M has been estimated, we can remove it from the data and proceed with the other PPS parameters, as already described.

IV. Performance Evaluation

We first derive the CRLB's for the PPS and FM parameters, and then we compare, based on Monte Carlo simulations, the proposed estimators with the CRLB's.

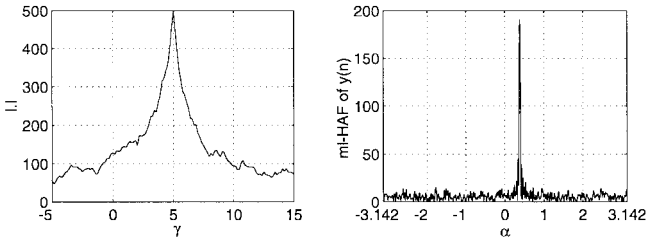

(a) (b)

Fig. 3. Plots for the estimation of (a) γ and (b) a_M.

A. Cramér–Rao Lower Bounds

Consider the PPS-FM model in (1), and denote the parameter vector as $\boldsymbol{\theta} := [\boldsymbol{\theta}_{\rm PPS}^T \boldsymbol{\theta}_{\rm FM}^T]^T$ for the log-likelihood function $\Lambda(\boldsymbol{\theta})$ given by (2). If $\hat{\boldsymbol{\theta}}$ is an unbiased estimator of $\boldsymbol{\theta}$, then it must satisfy $\mathrm{cov}(\hat{\boldsymbol{\theta}}) \geq \mathbf{J}^{-1}$, where $\mathbf{J}$ is the so-called Fisher information matrix (FIM). As a first step toward deriving the CRLB's, let us write the observed data in vector form as $\mathbf{x} = \mathbf{s}(\boldsymbol{\theta}) + \mathbf{v}$, where $[\mathbf{x}]_n := x(n)$, $n = 0, 1, \cdots, N-1$; similar definitions apply to $\mathbf{s}(\boldsymbol{\theta})$ and $\mathbf{v}$. Note the explicit dependence of the signal vector on the vector parameter $\boldsymbol{\theta}$. Due to the assumptions on $v(n)$, we have that $\mathbf{x}$ is an $N \times 1$ complex Gaussian circular vector with mean value $E\{\mathbf{x}\} = \mathbf{s}$ and covariance matrix $E\{\mathbf{x}\mathbf{x}^H\} = \sigma_v^2 \mathbf{I}$, where ^{H} denotes conjugate transpose, and $\mathbf{I}$ is an $N \times N$ identity matrix. Calculation of the FIM for a vector of correlated complex Gaussian observations is carried out in [13, ch. 3], and in our case, it produces for the (i, j)th entry

$$J_{ij} = \frac{2}{\sigma_v^2} \Re\left\{ \frac{\partial \mathbf{s}^H(\boldsymbol{\theta})}{\partial \theta_i} \frac{\partial \mathbf{s}(\boldsymbol{\theta})}{\partial \theta_j} \right\}. \tag{64}$$

The CRLB's are obtained from the diagonal elements of $\mathbf{J}^{-1}$, which we denote as $\mathrm{CRLB}(\theta_i) = [\mathbf{J}^{-1}]_{ii}$. Inserting $s(n)$ of (1) in (64) and taking partial derivatives, we obtain the elements of the FIM. As with Sections II and III, we will consider two FM models: the sinusoidal and the hyperbolic.

1) PPS-Sinusoidal FM: To avoid numerical problems in the inversion of the FIM, it is useful to redefine $\boldsymbol{\theta}_{\rm FM}$ and $\boldsymbol{\theta}_{\rm PPS}$ as

$$\begin{aligned} \boldsymbol{\theta}_{\rm FM} &:= [b \; N\omega_0 \; \phi_0]^T \\ \boldsymbol{\theta}_{\rm PPS} &:= [N^0 a_0 \; \cdots \; N^m a_m \; \cdots \; N^M a_M]^T. \end{aligned} \tag{65}$$

a) Exact CRLB's: Evaluation of J_{ij} is not difficult, but it is tedious. Skipping the details, we found that

$$J_{a_i, a_m} = \frac{8\pi^2\rho^2}{i!m!\,\sigma_v^2} \sum_{n=0}^{N-1} \left(\frac{n}{N}\right)^{i+m}, \quad (i, m) = 0, 1, \cdots, M \tag{66}$$

$$J_{b,b} = \frac{8\pi^2\rho^2}{\sigma_v^2} \sum_{n=0}^{N-1} \sin^2(\omega_0 n + \phi_0) \tag{67}$$

$$J_{\omega_0, \omega_0} = \frac{8\pi^2\rho^2 b^2}{\sigma_v^2} \sum_{n=0}^{N-1} \left(\frac{n}{N}\right)^2 \cos^2(\omega_0 n + \phi_0) \tag{68}$$

$$J_{\phi_0, \phi_0} = \frac{8\pi^2\rho^2 b^2}{\sigma_v^2} \sum_{n=0}^{N-1} \cos^2(\omega_0 n + \phi_0) \tag{69}$$

$$J_{a_i, b} = \frac{8\pi^2\rho^2}{i!\sigma_v^2} \sum_{n=0}^{N-1} \left(\frac{n}{N}\right)^i \sin(\omega_0 n + \phi_0) \tag{70}$$

$$J_{a_i, \omega_0} = \frac{8\pi^2\rho^2 b}{i!\sigma_v^2} \sum_{n=0}^{N-1} \left(\frac{n}{N}\right)^{i+1} \cos(\omega_0 n + \phi_0) \tag{71}$$

$$J_{a_i, \phi_0} = \frac{8\pi^2\rho^2 b}{i!\sigma_v^2} \sum_{n=0}^{N-1} \left(\frac{n}{N}\right)^i \cos(\omega_0 n + \phi_0) \tag{72}$$

$$J_{b, \omega_0} = \frac{4\pi^2\rho^2 b}{\sigma_v^2} \sum_{n=0}^{N-1} \left(\frac{n}{N}\right) \sin(2\omega_0 n + 2\phi_0) \tag{73}$$

$$J_{b, \phi_0} = \frac{4\pi^2\rho^2 b}{\sigma_v^2} \sum_{n=0}^{N-1} \sin(2\omega_0 n + 2\phi_0) \tag{74}$$

$$J_{\omega_0, \phi_0} = \frac{8\pi^2\rho^2 b^2}{\sigma_v^2} \sum_{n=0}^{N-1} \left(\frac{n}{N}\right) \cos^2(\omega_0 n + \phi_0). \tag{75}$$

Equations (66)–(75) allow the exact numerical evaluation of the FIM, but it is not clear how the parameters affect the bounds. However, a large sample approximation can be derived by regarding the sums as an Euler approximation of the integral $\sum_{n=0}^{N-1} f(n) \approx \int_0^N f(t)\,dt$. The same approach was used in [20] and was justified by noting that the PPS has bounded variation on any closed interval, which guarantees that the approximation is accurate. Large N expressions for the FIM of PPS parameters have been derived also in [25].

b) Approximate CRLB's for Large N: We adopt the following approximations:

$$\sum_{n=0}^{N-1} \left(\frac{n}{N}\right)^i \approx \int_0^N \left(\frac{t}{N}\right)^i dt = \frac{N}{i+1}$$

$$\begin{aligned} \sum_{n=0}^{N-1} \sin(\omega_0 n + \phi_0) &\approx \int_0^N \sin(\omega_0 t + \phi_0)\,dt \\ &= -\frac{\cos(\omega_0 N + \phi_0) - \cos(\phi_0)}{\omega_0}. \end{aligned}$$

For $i > 0$, we have

$$\begin{aligned} \sum_{n=0}^{N-1} \left(\frac{n}{N}\right)^i \sin(\omega_0 n + \phi_0) &\approx \int_0^N \left(\frac{t}{N}\right)^i \sin(\omega_0 t + \phi_0)\,dt \\ &= -\frac{\cos(\omega_0 N + \phi_0)}{\omega_0} + O(N^{-1}) \end{aligned}$$

$$\begin{aligned} \sum_{n=0}^{N-1} \left(\frac{n}{N}\right)^i \cos(\omega_0 n + \phi_0) &\approx \int_0^N \left(\frac{t}{N}\right)^i \cos(\omega_0 t + \phi_0)\,dt \\ &= \frac{\sin(\omega_0 N + \phi_0)}{\omega_0} + O(N^{-1}) \end{aligned}$$

where we have used the Landau's notation

$$f(N) = O(N) \overset{\rm def}{\Longleftrightarrow} \lim_{N\to\infty} \frac{f(N)}{N} = c, \quad 0 < |c| < \infty. \tag{76}$$

Equations (66)–(75) can be approximated by

$$J_{a_i,a_m} := \frac{8\pi^2\rho^2}{(i+m+1)i!m!\,\sigma_v^2} \tag{77}$$

$$J_{b,b} := \frac{4\pi^2\rho^2}{\sigma_v^2}\left[N - \frac{\sin(2\omega_0 N+2\phi_0)-\sin(2\phi_0)}{\omega_0}\right] \tag{78}$$

$$J_{\omega_0,\omega_0} := \frac{4\pi^2\rho^2 b^2}{\sigma_v^2}\left[\frac{N}{3} + \frac{\sin(2\omega_0 N+2\phi_0)}{\omega_0}\right] \tag{79}$$

$$J_{\phi_0,\phi_0} := \frac{4\pi^2\rho^2 b^2}{\sigma_v^2}\left[N + \frac{\sin(2\omega_0 N+2\phi_0)-\sin(2\phi_0)}{\omega_0}\right] \tag{80}$$

$$J_{a_0,b} := -\frac{8\pi^2\rho^2}{i!\sigma_v^2}\cdot\frac{\cos(\omega_0 N+\phi_0)-\cos(\phi_0)}{\omega_0} \tag{81}$$

$$J_{a_i,b} := -\frac{8\pi^2\rho^2}{i!\sigma_v^2}\cdot\frac{\cos(\omega_0 N+\phi_0)}{\omega_0}, \qquad 1\le i\le M \tag{82}$$

$$J_{a_i,\omega_0} := \frac{8\pi^2\rho^2 b}{i!\sigma_v^2}\cdot\frac{\sin(\omega_0 N+\phi_0)}{\omega_0} \tag{83}$$

$$J_{a_0,\phi_0} := \frac{8\pi^2\rho^2 b}{\sigma_v^2}\cdot\frac{\sin(\omega_0 N+\phi_0)-\sin(\phi_0)}{\omega_0} \tag{84}$$

$$J_{a_i,\phi_0} := \frac{8\pi^2\rho^2 b}{i!\sigma_v^2}\cdot\frac{\sin(\omega_0 N+\phi_0)}{\omega_0}, \qquad 1\le i\le M \tag{85}$$

$$J_{b,\omega_0} := -\frac{4\pi^2\rho^2 b}{\sigma_v^2}\cdot\frac{\cos(2\omega_0 N+2\phi_0)}{2\omega_0} \tag{86}$$

$$J_{b,\phi_0} := -\frac{4\pi^2\rho^2 b}{\sigma_v^2}\cdot\frac{\cos(2\omega_0 N+2\phi_0)-\cos(2\phi_0)}{2\omega_0} \tag{87}$$

$$J_{\omega_0,\phi_0} := \frac{2\pi^2\rho^2 b^2}{\sigma_v^2}\left[N + \frac{\sin(2\omega_0 N+2\phi_0)}{\omega_0}\right]. \tag{88}$$

The FIM can be written as

$$\mathbf{J} = \begin{bmatrix}\mathbf{A} & \mathbf{C}\\ \mathbf{C}^T & \mathbf{F}\end{bmatrix} \tag{89}$$

where $\mathbf{A}$ is a square $(M+1)\times(M+1)$ matrix with elements $[\mathbf{A}]_{i+1,m+1} := J_{a_i,a_m}$, with $0\le i,m\le M$; $\mathbf{F}$ is a square 3×3 matrix given by

$$\mathbf{F} := \begin{bmatrix} J_{b,b} & J_{b,\omega_0} & J_{b,\phi_0}\\ J_{b,\omega_0} & J_{\omega_0,\omega_0} & J_{\omega_0,\phi_0}\\ J_{b,\phi_0} & J_{\omega_0,\phi_0} & J_{\phi_0,\phi_0}\end{bmatrix}. \tag{90}$$

Matrix $\mathbf{C}$ is $(M+1)\times 3$, containing all the cross-elements, i.e., $[\mathbf{C}]_{i+1,1} := J_{a_i,b}$, $[\mathbf{C}]_{i+1,2} := J_{a_i,\omega_0}$, $[\mathbf{C}]_{i+1,3} := J_{a_i,\phi_0}$. By using the partitioned matrix inversion formula, the Cramér–Rao inequality results as in (91), shown at the bottom of the page.

In Fig. 4, the CRLB's of the FM and PPS parameters are reported for SNR = 12 dB, $b=0.05$, $\omega_0=0.015$, and $\phi_0=0$. Note that the values of the PPS parameters do not affect the bounds. The solid and dashed lines refer to the exact and approximate CRLB's, respectively. The dash-dotted lines refer to the exact CRLB's when only FM or only PPS parameters are present (let us call them marginal CRLB's), given by the diagonal elements of $\mathbf{F}^{-1}$ and $\mathbf{A}^{-1}$, respectively. Note that according to (65), here, CRLB(a_m) denotes the bound of $N^m a_m$; therefore, the variance of any unbiased estimator of a_m satisfies var$\{\hat{a}_m\} \ge N^{-2m}$CRLB$(a_m)$. Similarly, from (65), we have var$\{\hat{\omega}_0\} \ge N^{-2}$CRLB$(\omega_0)$. As we see, asymptotic behavior is reached at about $N=1000$. Note that all the CRLB's decrease linearly both with respect to the SNR and w.r.t. N (in agreement with the known result that asymptotically the Cramér–Rao bound of a_m shows a decreasing rate of N^{2m+1} [25], [26]). The effect of the coupling between the PPS and the FM parameters is evident by comparing the plots with solid and dash-dotted lines. The results show that for $N>1000$, the coupling tends to be negligible. How "negligible" the coupling is, e.g., for b, becomes evident from Fig. 5(a), which was obtained for $N=2048$ and various values of b. We also observed that while the CRLB's of b [Fig. 5(a)] and of all the a_i's do not depend on the modulation index, the CRLB's of ω_0 [Fig. 5(b)] and ϕ_0 decrease proportionally to b^2.

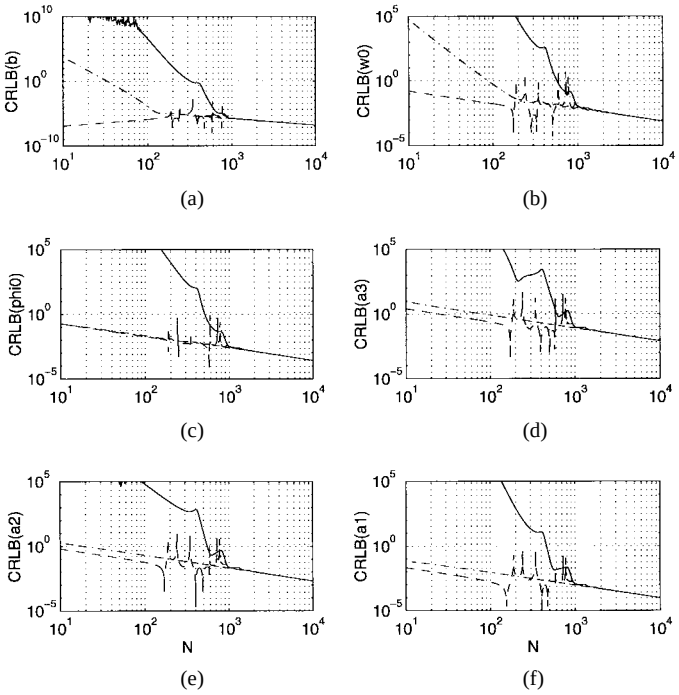

Fig. 4. Exact (solid), approximate (dashed), and marginal (dash-dotted) CRLB's versus N.

2) PPS-Hyperbolic FM: In this case, $\phi_{\rm FM}(n) = 2\pi\gamma\ln(n)$; therefore, $\boldsymbol{\theta}_{\rm FM}$ is the scalar parameter $\theta_{\rm FM} := \gamma$. Matrix $\mathbf{F}$ in (90) reduces to a scalar $J_{\gamma,\gamma}$, and $\mathbf{C}$ becomes an $(M+1)\times 1$ vector with elements $J_{a_i,\gamma}$. Taking partial

$$\mathrm{cov}(\hat{\boldsymbol{\theta}}) \ge \mathbf{J}^{-1} = \begin{bmatrix}(\mathbf{A}-\mathbf{C}\mathbf{F}^{-1}\mathbf{C}^T)^{-1} & -(\mathbf{A}-\mathbf{C}\mathbf{F}^{-1}\mathbf{C}^T)^{-1}\mathbf{C}\mathbf{F}^{-1}\\ -(\mathbf{F}-\mathbf{C}^T\mathbf{A}^{-1}\mathbf{C})^{-1}\mathbf{C}^T\mathbf{A}^{-1} & (\mathbf{F}-\mathbf{C}^T\mathbf{A}^{-1}\mathbf{C})^{-1}\end{bmatrix} \tag{91}$$

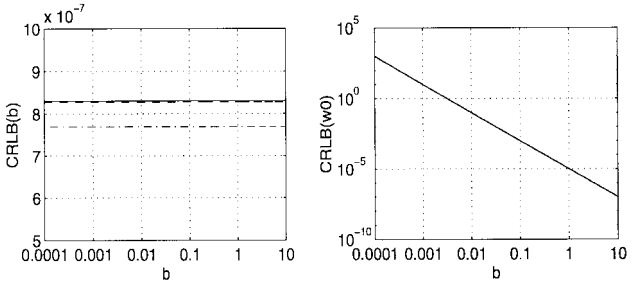

(a) (b)

Fig. 5. Exact (solid), approximate (dashed), and marginal (dash-dotted) CRLB's versus b.

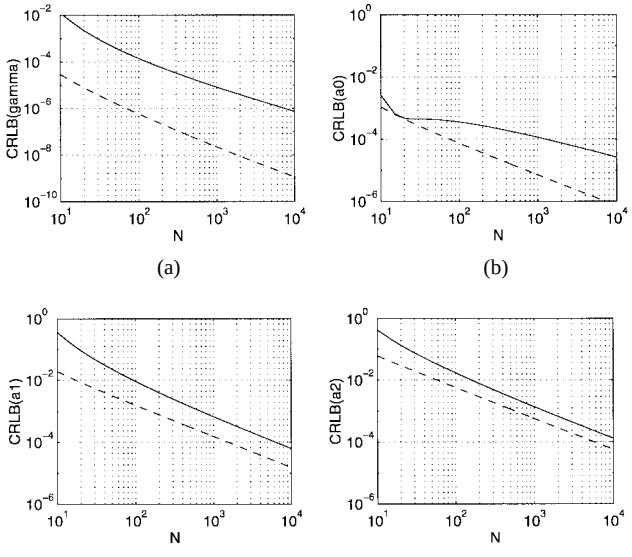

(a) (b) (c) (d)

Fig. 6. Exact (solid) and marginal (dashed) CRLB's versus N.

derivatives in (64), we obtain

$$J_{\gamma,\gamma} = \frac{8\pi^2\rho^2}{\sigma_v^2} \sum_{n=1}^{N} \ln^2(n) \tag{92}$$

$$J_{a_i,\gamma} = \frac{8\pi^2\rho^2}{i!\sigma_v^2} \sum_{n=1}^{N} \left(\frac{n}{N}\right)^i \ln(n), \qquad i = 0, 1, \cdots, M \tag{93}$$

where the two sums range from 1 to N to avoid $\ln(0)$. Defining the $(M+1)\times 1$ vector $\mathbf{c} := [J_{a_0,\gamma}\ J_{a_1,\gamma}\ \cdots\ J_{a_M,\gamma}]^T$, we find the CRLB as in (94), shown at the bottom of the page.

From (92) and (93), we derive that the CRLB's are not affected by the values of γ and $\{a_m\}_{m=0}^{M}$. Fig. 6 shows the CRLB's of the FM parameter γ and of the PPS parameters for SNR $= 12$ dB. The solid and dashed lines refer to the exact and marginal CRLB's given by $1/J_{\gamma,\gamma}$ and by the diagonal elements of $\mathbf{A}^{-1}$, respectively. In this case, the coupling effect between the γ and $\{a_m\}$ seems to be not negligible, even for large N.

3) CRLB's for ρ and σ_v^2: When ρ and σ_v^2 are also unknown, we could be interested in deriving their CRLB's. We omit the details of the derivation, but it can be easily found to be $J_{\rho,\rho} = 2N/\sigma_v^2$, $J_{\sigma_v^2,\sigma_v^2} = N/\sigma_v^4$; the cross-elements of the FIM are zero, i.e., $J_{\rho,\theta_i} = J_{\sigma_v^2,\theta_i} = 0$, $\forall i$. This implies that CRLB$(\rho) = \sigma_v^2/(2N)$, CRLB$(\sigma_v^2) = \sigma_v^4/N$, and bounds for ρ and σ_v^2 are decoupled from those of the PPS and FM parameters derived previously.

B. Simulations and Comparisons with the CRLB's

To illustrate and evaluate the various parameter estimation algorithms discussed so far, we simulated numerically the performance by Monte Carlo experiments, and we compared them with the CRLB's.

Example 1—Narrowband FM Signal and Third-Order PPS: We first generated $N = 2048$ samples according to (1), with $\phi_{\mathrm{FM}}(n) = 2\pi b \sin(\omega_0 n + \phi_0)$ and parameters $\rho = 1$, $b = 0.05$, $\omega_0 = 0.015$, $\phi_0 = 0$, $a_0 = 0$, $a_1 = 0.25$, $a_2 = 1.3889 \cdot 10^{-3}$, $a_3 = 1.3022 \cdot 10^{-5}$. The noise variance σ_v^2 was set to obtain the desired signal-to-noise ratio, which was defined as SNR $:= \rho^2/\sigma_v^2$. The sets of lags in the product ml-HAF were $(\tau_{1,l},\ \tau_{2,l}) = (60, 60)$, $(72, 50)$, $(75, 48)$, $(80, 45)$, $(90, 40)$, and $(100, 36)$ so that $\tau_{1,l} \cdot \tau_{2,l} = 3600$ for $l = 1, \cdots, 6$; consequently, $\omega_c = 1.1782$ and $\beta_l = 0.7711, 0.7555, 0.7476, 0.7319, 0.6923$, and 0.6445, respectively. Note that all of them are less than one so that the second-order approximation (21) is accurate, and β can be estimated via (49). In Fig. 2(b), the product ml-HAF is plotted for SNR $= 12$ dB. It peaks (theoretically) at $\{\omega_c + k\omega_0\}_{k=-2}^{2} = \{1.1782 + 0.015 \cdot k\}_{k=-2}^{2}$. Fig. 2(c) and (d) show, respectively, the second-order HAF of $x_1(n)$ in (46) and the DFT of $x_2(n)$ in (48). They exhibit a sharp peak at $\alpha = 4\pi\tau_1 a_2 = 1.7453$ ($\tau_1 = \tau_{1,6} = 100$), and $\alpha = 2\pi a_1 = 1.5708$, respectively. As described in Section III, from the peaks' location of the plots in Fig. 2(b)–(d), we derive the estimates of ω_0, a_3, a_2, and a_1.

The maximum was found by two successive 1-D searches. The first coarse search was implemented by using FFT (the signal was zero-padded to $N_{zp} = 4096$ points). Then, a fine search was performed in an identical manner by using the chirp Fourier transform algorithm [20] to search around the maximum found by the previous coarse search. The final resolution obtained in this manner is about N_{zp}^{-2}.

In Fig. 7, we show the error variance of the estimates versus SNR, obtained from 1000 independent Monte Carlo runs (in each run, we generated $N = 2048$ samples). The solid lines refer to the exact CRLB's [CRLB(ω_0) and CRLB(a_m) were properly scaled by N^2 and N^{2m}, respectively]; the dashed lines correspond to the case of known amplitude ρ; the x marks refer to the case where ρ is unknown and is estimated jointly with the noise power σ_v^2 according to (52) and (53). In the range of SNR's investigated, no sensible difference was observed between the two cases (known ρ and unknown ρ),

$$\mathrm{cov}(\hat{\boldsymbol{\theta}}) \geq \mathbf{J}^{-1} = \begin{bmatrix} (\mathbf{A} - \mathbf{c}\mathbf{c}^T/J_{\gamma,\gamma})^{-1} & -(\mathbf{A} - \mathbf{c}\mathbf{c}^T/J_{\gamma,\gamma})^{-1}\mathbf{c}/J_{\gamma,\gamma} \\ -(J_{\gamma,\gamma} - \mathbf{c}^T\mathbf{A}^{-1}\mathbf{c})^{-1}\mathbf{c}^T\mathbf{A}^{-1} & (J_{\gamma,\gamma} - \mathbf{c}^T\mathbf{A}^{-1}\mathbf{c})^{-1} \end{bmatrix} \tag{94}$$

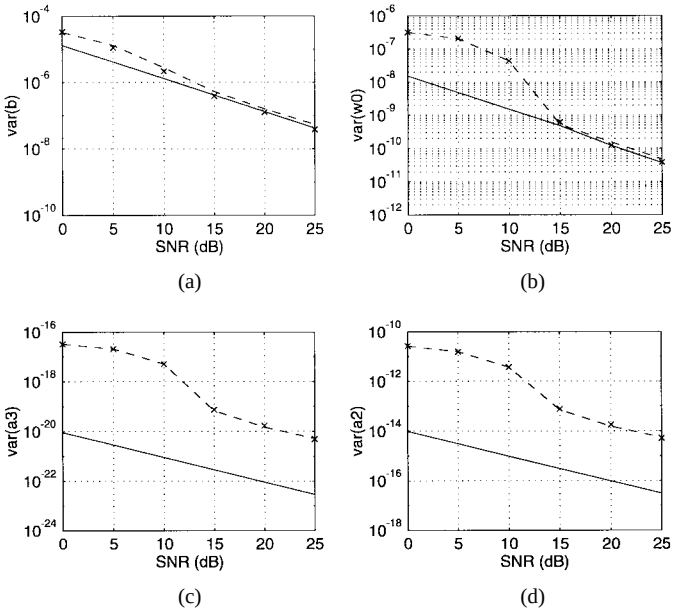

Fig. 7. Error variance for known ρ (dashed), unknown ρ (x marks), and CRLB's (solid) versus SNR.

TABLE I
BIASED FOR UNKNOWN ρ

$SNR(dB)$	bias($\hat{b}$)	bias($\hat{\omega}_0$)	bias($\hat{a}_2$)	bias($\hat{a}_3$)
0	$1.0390 \cdot 10^{-2}$	$-4.3649 \cdot 10^{-4}$	$-1.5316 \cdot 10^{-6}$	$1.7771 \cdot 10^{-9}$
5	$5.3407 \cdot 10^{-3}$	$-5.6142 \cdot 10^{-4}$	$-2.4783 \cdot 10^{-6}$	$2.5734 \cdot 10^{-9}$
10	$2.9554 \cdot 10^{-3}$	$-2.4511 \cdot 10^{-4}$	$-3.6245 \cdot 10^{-6}$	$3.5445 \cdot 10^{-9}$
15	$2.4478 \cdot 10^{-3}$	$-1.6849 \cdot 10^{-4}$	$-3.9477 \cdot 10^{-6}$	$3.8485 \cdot 10^{-9}$
20	$2.3982 \cdot 10^{-3}$	$-1.6782 \cdot 10^{-4}$	$-3.9409 \cdot 10^{-6}$	$3.8423 \cdot 10^{-9}$
25	$2.4068 \cdot 10^{-3}$	$-1.6794 \cdot 10^{-4}$	$-3.9481 \cdot 10^{-6}$	$3.8491 \cdot 10^{-9}$

except for $\hat{b}$. In fact, Fig. 7(a) shows that the error variance for unknown ρ is slightly below the error variance for known ρ. This phenomenon has already been discussed in [10]; in particular, it is proved that when we used the maximum likelihood approach or the method of moments approach, the error variance may decrease when parameters of interest (in this case b) are jointly estimated with *nuisance* parameters (in this case ρ), with respect to the case where the nuisance parameters are perfectly known. We also note that the error variances of $\hat{a}_3$ and $\hat{a}_2$ are not very close to the bounds.

Table I shows the biases of the estimates for unknown ρ.

The results in Table I tell us that the bias is not generally negligible with respect to error standard deviation; therefore, it affects the mse. Probably, the main reason for this lack of consistency is due to the fact that the estimation algorithm for narrowband FM signals is based on (22), that is, only approximately valid. Estimation accuracy could improve by considering terms of order higher than the second in (21). Along this direction, the cost to be paid is in terms of computational complexity; it would be more complicated to recover β from the amplitude of the HAF at the peaks. In part, the results in Fig. 7 can also be due to the fact that even when the FM component is not present, the estimates of $\{a_m\}$ are slightly biased (even in the absence of noise [20]). According to [20], this bias is inversely proportional to N^2. Another reason may be related to the limited amount of zero padding; unfortunately, simulations with larger values of N_{ZP} would be too computationally demanding.

In any case, it is worth stressing that the mse, even if it is not close to the CRLB, is still much lower than the true values of the parameters ($a_2 = 1.3889 \cdot 10^{-3}$ and $a_3 = 0.13022 \cdot 10^{-5}$), and this can be more than enough in some applications (e.g., for target classification purposes). Alternatively, if we are willing to trade off more computations for optimality, the suboptimal solutions can be used to initialize a nonlinear least-squares (NLLS) matching algorithm in order to speed up the search required by any NLLS method and prevent convergence to local minima. Specifically, we could treat $\hat{s}_M(n; \boldsymbol{\tau_l})$ as "data" and minimize, with respect to $\boldsymbol{\theta}_r := [\beta, \omega_c, \omega_0, \psi_c, \psi_0]$, the following statistic:

$$P_N(\boldsymbol{\theta}_r) := \sum_{n=1}^{N} |\hat{s}_M(n; \boldsymbol{\tau_l}) - s_M(n; \boldsymbol{\tau_l})|^2. \tag{95}$$

Recalling (17), $\hat{s}_M(n; \boldsymbol{\tau_l}) = x_M(n; \boldsymbol{\tau_l})$, and after straightforward manipulations, estimation of $\boldsymbol{\theta}_r$ reduces to

$$\hat{\boldsymbol{\theta}}_r = \arg \max_{\theta_r} \cdot \left| \sum_{n=1}^{N} x_M(n; \boldsymbol{\tau_l}) \sum_{k=-K}^{K} J_k(\beta) e^{j[(\omega_c + k\omega_0)n + \psi_c + k\psi_0]} \right| \tag{96}$$

that must be solved by nonlinear optimization. Mean square consistency of the NLLS estimator follows from the white Gaussian noise assumption. However, investigation of the performance of estimator (96) is beyond the scope of this work.

Example 2—Wideband FM Signal and Second-Order PPS: Here, we generated $N = 1024$ samples of the FM-PPS process with second-order polynomial phase and parameters given by $b = 6$, $\omega_0 = 0.0491$, $\phi_0 = 0$, $a_0 = 0.5$, $a_1 = 0.1$, $a_2 = 3.4722 \cdot 10^{-4}$, and $\tau_1 = 129$; therefore, $\omega_c = 0.5629$ and $\beta = 3.6996$. In Fig. 1(b), the ml-HAF $X_2(\alpha; \tau_1)$ is plotted for SNR $= 16$ dB versus $\alpha \in [0, 1]$. From the location and value of the peaks, we derive our estimates. The modulation index was estimated according to the method reported in (39), which was proposed in [27]. Note that $\beta > 1$, and therefore, we cannot use (49). Table II shows biases and variances of the estimates for the SNR $= 16$ dB (first two rows) and 8 dB (last two rows) obtained from 400 independent Monte Carlo runs ($N = 1024$ samples per run). It was observed in [27] that although (16) holds for any s, different s in (39) result in different estimates of β. The performance of $\hat{\beta}$ as a function of s was studied in [27] by Monte Carlo simulations with the ultimate goal of finding the optimal choice of s. By making use of those results (see e.g., [27, Fig. 3]), we set $s = 2.75$.

As we see from Table II, low SNR increases the variance of b. Even if the estimator (39) guarantees reliable estimates of the modulation index for a pure FM tone observed in additive white Gaussian noise, when it is applied to the "data" $x_M(n; \boldsymbol{\tau_l})$ all the cross-terms between $s(n)$ and $v(n)$ present in the ml-HIM of $x(n)$ contribute to the disturbance term, which, consequently, can no longer be considered white

TABLE II
FM-PPS PARAMETERS (SNR = 16 dB AND 8 dB)—METHOD OF [27]

	$\hat{b}$	$\hat{\omega}_0$	$\hat{\psi}_0$	$\hat{a}_2$	$\hat{a}_1$	$\hat{a}_0$
Bias	-1.3579	$-1.9890 \cdot 10^{-5}$	0.0574	$-1.8236 \cdot 10^{-8}$	0.0174	-0.2938
Var	0.0460	$2.7497 \cdot 10^{-10}$	$4.7490 \cdot 10^{-5}$	$2.327 \cdot 10^{-15}$	0.0028	0.0376
Bias	-4.1559	$-7.6639 \cdot 10^{-5}$	0.0549	$-4.3700 \cdot 10^{-7}$	-0.0226	-0.4019
Var	$1.1172 \cdot 10^{4}$	$3.1892 \cdot 10^{-8}$	0.0106	$5.6254 \cdot 10^{-13}$	0.0276	0.0765

TABLE III
FM-PPS PARAMETERS (SNR = 16 dB AND 8 dB)—METHOD OF [12]

	$\hat{b}$	$\hat{\omega}_0$	$\hat{\psi}_0$	$\hat{a}_2$	$\hat{a}_1$	$\hat{a}_0$
Bias	0.1805	$-2.1330 \cdot 10^{-5}$	-0.15128	$-1.7368 \cdot 10^{-8}$	-7.0361	-0.5417
Var	0.0728	$2.3860 \cdot 10^{-10}$	$4.4781 \cdot 10^{-5}$	$2.2164 \cdot 10^{-15}$	0.1595	$7.4281 \cdot 10^{-2}$
Bias	-1.5891	$-5.5421 \cdot 10^{-5}$	-0.1507	$-2.8428 \cdot 10^{-8}$	-0.1058	-0.4967
Var	$7.5791 \cdot 10^{3}$	$3.4980 \cdot 10^{-8}$	$1.2378 \cdot 10^{-2}$	$5.7722 \cdot 10^{-13}$	$1.4172 \cdot 10^{-1}$	$8.2668 \cdot 10^{-2}$

or Gaussian. This seems to have deleterious effects on the performance of (39), as shown in Table II. A possible remedy is to use the estimate ω_0 to select a new set of lags in such a way that $\beta < 1$ and then estimate b via (49). We repeated the simulations, this time with $\tau_1 = 256$, so that $\beta = 0.2435$, and we obtained bias$(\hat{b}) = 0.1384$, var$(\hat{b}) = 0.6407$ for SNR $= 16$ dB, and bias$(\hat{b}) = 0.1469$, var$(\hat{b}) = 3.0400$ for SNR $=$ 8 dB. The improvement in accuracy (at least for the low SNR case) is now noticeable.

We also implemented the method based on (40) to estimate the modulation index. The results reported in Table III show that the two methods exhibit comparable performance.

Example 3—Hyperbolic FM Signal and Second-Order PPS: We generated samples of $x(n)$ according to (29) for a second-order PPS (a chirp) multiplied by a hyperbolic FM with parameters $\rho = 1$, $\gamma = 5$, $a_0 = 0.1$, $a_1 = 0.25$, $a_2 = 1.0208 \cdot 10^{-3}$. The sets of lags used to calculate the ml-HIM $x_{M+1}(n; \boldsymbol{\tau}_l)$ in (56) were $(\tau_{1,l}, \tau_{2,l}) = (60, 60), (72, 50), (75, 48), (80, 45), (90, 40), (100, 36)$ when $N = 512$; $(\tau_{1,l}, \tau_{2,l}) = (30, 30), (36, 25), (45, 20), (50, 18)$ when $N = 256$; $(\tau_{1,l}, \tau_{2,l}) = (15, 15), (25, 9)$, when $N = 128$; $(\tau_{1,l}, \tau_{2,l}) = (8, 8), (16, 4)$, when $N = 64$; and $(\tau_{1,l}, \tau_{2,l}) = (4, 4), (8, 2)$ when $N = 32$. To estimate γ, we applied the algorithm in (56). With respect to the ML approach, estimator (56) decouples the problem of estimating γ from that of estimating $\{a_m\}$ and involves a 1-D search over γ [see Fig. 3(a)]. The maximum was found by two successive 1-D searches: one over a coarse grid of $N_\gamma = 129$ points and a second over a fine grid. Therefore, the final resolution obtained is $N_\gamma^{-2} = 6.0093 \cdot 10^{-5}$. Alternatively, more sophisticated maximization techniques can be used, like a Newton–Raphson or a scoring algorithm (see [6] or [13]).

In Fig. 8(a), we plot the mean square error of $\hat{\gamma}$ (x marks), $\hat{a}_1$ (circles), $\hat{a}_2$ (stars) versus the sample size N obtained from 500 independent Monte Carlo runs. The signal-to-noise ratio was SNR $= 10$ dB. The solid, dash-dotted, and dashed lines refer to the corresponding CRLB's [with CRLB(a_m) properly scaled by N^{2m}]. The other plots show the mse of $\hat{\gamma}$ [Fig. 8(b)], $\hat{a}_1$ [Fig. 8(c)], and $\hat{a}_2$ [Fig. 8(d)] versus SNR for $N = 256$ (x marks) and $N = 512$ (circles). The corresponding CRLB's are also shown for comparison (solid line for $N = 256$ and dash-dotted line for $N = 512$). The performance of the proposed estimators is satisfactory and close to the CRLB's. The SNR above, during which the proposed estimators begin to track the CRLB's, is approximately 5 dB. It is worth stressing that relative to [16] and [17], the proposed method considers not only the first-order PPS parameter a_1 (that takes into account the Doppler shift due to a constant radial velocity) but also all the remaining $\{a_m\}$'s; it is therefore applicable to more general target motions. Other advantages are the following.

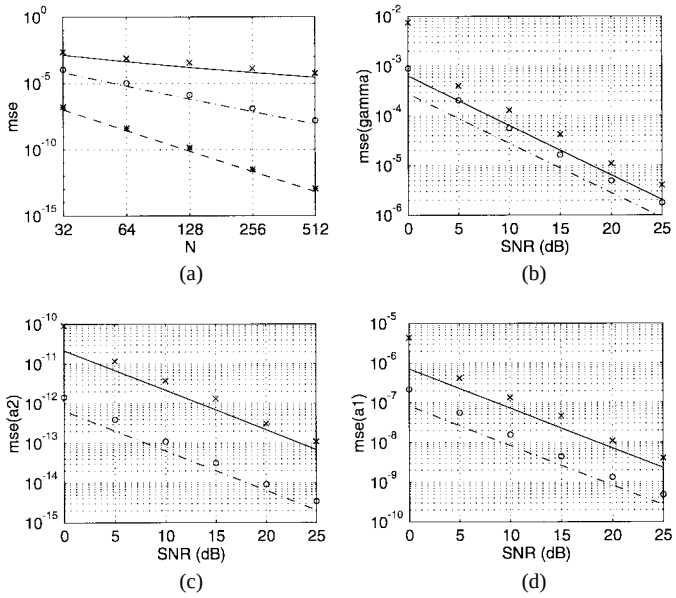

Fig. 8. (a) Mean square error of $\hat{\gamma}$ (x-marks), $\hat{a}_1$ (circles), $\hat{a}_2$ (stars), and CRLB's (solid, dash-dotted, dashed line, respectively) versus the sample size N. MSE of (b) $\hat{\gamma}$, (c) $\hat{a}_2$, and (d) $\hat{a}_1$ versus SNR for $N = 256$ (x-marks) and $N = 512$ (circles). The corresponding CRLB's are also shown as a comparison with solid line for $N = 256$ and dash-dotted line for $N = 512$.

i) It does not require phase unwrapping.
ii) The allowable range of γ is not constrained to be small (e.g., in [16], we must have $|\gamma| < 1.7$ when $a_1 = 0$).
iii) The algorithm's performance is close to the CRLB's for SNR thresholds above 5 dB, instead of the 12 dB reported in [16].

V. Conclusions

Parameter estimation of a class of nonstationary complex signals whose phase can be modeled as a superposition of a polynomial term and a nonlinear (sinusoidal or hyperbolic) frequency modulated term was addressed. Previously proposed methods for estimating the FM parameters (and, in particular, the modulation index) do not include PPS components, and, vice-versa, the standard approach based on the HAF for PPS parameter estimation cannot work when the FM component is present. The proposed method handles the more general scenario of hybrid FM-PPS signals exploiting the properties of the multilag HAF. This approach allows us to decouple estimation of the FM parameters from that of the PPS with a noticeable reduction in computational complexity. The redundancy offered by the multilags can also be used to reduce the FM term to a narrowband process and thereby improves the accuracy of the modulation index estimation. The exact Fisher information matrix for the FM-PPS parameters and an asymptotic form of the CRLB's were derived. Computer simulations were carried out to compare the performance of the proposed methods with the relevant CRLB's.

The model adopted herein is potentially useful for practical radar/sonar modeling and target classification. A direction for future research is to generalize the signal model in order to consider general periodic FM ($\phi_{\rm FM}(n) = p(n)$ with $p(n)$ a periodic signal), possibly with random or deterministic periodically time-varying amplitude. In fact, in some cases of practical interest, it would be oversimplifying to assume that the phase modulation due to complicated phenomena (such as the jet engine modulation or the scattering from an helicopter main and tail rotors) can be realistically modeled as a single sinusoid (see [7] or [15] for a discussion on this point). The general periodic FM scenario includes the hybrid FM-PPS considered in this paper but presents additional challenges due to the presence of cross-terms among different sinusoids. As a final remark, the monocomponent model we assumed throughout the work is a good model for the echo from a point-like rotating target moving in a generic direction and observed by a coherent radar. In the more complex situation, where the radar resolution is high enough to resolve a certain number of scatterers, a multicomponent model would be more appropriate [4]. In this case, we could extend the approach based on the product multilag HAF, which was recently proposed in [5] for a multicomponent PPS scenario, to multicomponent hybrid FM-PPS signals. Results in this direction will be reported in future works.

Appendix
Proof of (62)

We need the following lemma due to Hasan [11].

Lemma 1 [11]: Let

$$S_{f^N}^N(\alpha) := \frac{1}{N}\sum_{n=0}^{N-1} f^N\left(\frac{n}{N}\right) e^{j\alpha n} \tag{97}$$

where $f^N(t)$ is a continuous function converging uniformly to $f(t)$ when N goes to infinity. Then

$$\lim_{N\to\infty} S_{f^N}^N(\alpha) = \left[\int_0^1 f(t)\,dt\right]\delta(\alpha). \tag{98}$$

We will make use of this lemma to show that $\lim_{N\to\infty} \hat{S}_M^{\rm FM}(\alpha;\boldsymbol{\tau_l}) = \delta(\alpha)$. For the sake of simplicity, consider the case $M = 2$. We want to evaluate

$$\lim_{N\to\infty} \hat{S}_2^{\rm FM}(\alpha;\tau_1) = \lim_{N\to\infty}\frac{1}{N}\sum_{n=\tau_1+1}^{N-\tau_1} \exp\left(j2\pi\gamma_e \ln\left[\frac{n+\tau_1}{n-\tau_1}\right]\right)e^{-j\alpha n} \tag{99}$$

where in writing the summation range, we have taken into account that we are dealing with finite sample size; therefore, $y(n+\tau_1)y^*(n-\tau_1) = 0$ for $n \le \tau_1$, and $n > N-\tau_1$. Changing the summation variable, we have

$$\hat{S}_2^{\rm FM}(\alpha;\tau_1) = \frac{1}{N}\sum_{n=0}^{N-2\tau_1-1} \times \exp\left(j2\pi\gamma_e \ln\left[\frac{n/N+2\tau_1/N}{n/N+1/N}\right]\right) \times e^{-j\alpha n}\, e^{j\alpha(\tau_1+1)}. \tag{100}$$

Now, define

$$f^N(t) := \exp\left[j2\pi\gamma \ln\left(\frac{t+2\tau_1/N}{t+1/N}\right)\right].$$

For every N, $f^N(t)$ is continuous in $t \in [0, 1]$ and for fixed τ_1 converges uniformly to $f(t) = \lim_{N\to\infty} f^N(t) = 1$, $\forall t \in [0, 1]$; hence, from Lemma 1 we have

$$\lim_{N\to\infty} \hat{S}_2^{\rm FM}(\alpha;\tau_1) = \lim_{N\to\infty}\frac{1}{N}\sum_{n=0}^{N-2\tau_1-1} f^N\left(\frac{n}{N}\right)e^{-j\alpha n} = \int_0^1 f(t)\,dt\cdot\delta(\alpha) = \delta(\alpha). \tag{101}$$

Inserting (101) in (61), we obtain (62). The result can be extended to general M by defining $f^N(t) := \exp[j2\pi\gamma_e \ln g_M(n;\boldsymbol{\tau_l})]$.

Acknowledgment

The authors would like to thank Prof. G. T. Zhou for kindly providing the software used in [27], which was useful in deriving part of the results reported in Example 2. Thanks also to Prof. A. Farina for bringing our attention to [7], for kindly providing [15], and for useful comments; and thanks to Dr. O. Besson for useful comments in a private correspondence.

References

[1] S. Barbarossa, "Detection and estimation of the instantaneous frequency of polynomial phase signals by multilinear time-frequency representations," in *Proc. IEEE-SP Workshop Higher Order Stat.*, Lake Tahoe, CA, June 1993, pp. 168–172.

[2] S. Barbarossa, A. Porchia, and A. Scaglione, "Multiplicative multilag higher-order ambiguity function," in *Proc. Int. Conf. Acoust., Speech, Signal Process.*, Atlanta, GA, May 1996, vol. 5, pp. 3022–3025.

[3] S. Barbarossa and O. Lemoine, "Analysis of nonlinear FM signals by pattern recognition of their time-frequency representation," *IEEE Signal Processing Lett.*, vol. 3, pp. 112–115, Apr. 1996.

[4] S. Barbarossa and A. Scaglione, "Motion compensation and target classification based on parametric modeling of the instantaneous frequency of echoes backscattered from rigid bodies," in *Proc. 31st Asilomar*

Conf. Signals, Syst., Comput., Pacific Grove, CA, Nov. 2–5, 1997, pp. 260–264.
[5] S. Barbarossa, A. Scaglione, and G. B. Giannakis, "Product multilag high-order ambiguity function for multicomponent polynomial phase signal modeling," *IEEE Trans. Signal Processing*, vol. 46, pp. 691–708, Mar. 1998.
[6] Y. Bard, *Nonlinear Parameter Estimation.* New York: Academic, 1974.
[7] M. R. Bell and R. A. Grubbs, "JEM modeling and measurement for radar target identification," *IEEE Trans. Aerosp. Electron. Syst.*, vol. 29, pp. 73–87, Jan. 1993.
[8] D. R. Brillinger, *Time Series: Data Analysis and Theory.* San Francisco, CA: Holden-Day, 1981.
[9] C. Corduneanu, *Almost Periodic Functions.* New York: Wiley, 1968.
[10] F. Gini, "Estimation strategies in the presence of nuisance parameters," *Signal Process.*, vol. 55, no. 2, pp. 241–245, 1996.
[11] T. Hasan, "Nonlinear time series regression for a class of amplitude modulated cosinusoids," *J. Time Series Anal.*, vol. 3, no. 2, pp. 109–122, 1982.
[12] S.-R. Huang, R. M. Lerner, and K. J. Parker, "On estimating the amplitude of harmonic vibration from the Doppler spectrum of reflected signals," *J. Acoust. Soc. Amer.*, vol. 88, pp. 2702–2712, Dec. 1990.
[13] S. M. Kay, *Fundamentals of Statistical Signal Processing: Estimation Theory.* Englewood Cliffs, NJ: Prentice-Hall, 1993.
[14] R. Kumaresan and S. Verma, "On estimating the parameters of chirp signals using rank reduction techniques," in *Proc. 21st Asilomar Conf. Signals, Syst., Comput.*, Pacific Grove, CA, 1987, pp. 555–558.
[15] S. Palumbo, S. Barbarossa, A. Farina, and M. R. Toma, "Classification techniques of radar signals backscattered by helicopter blades," in *Proc. Int. Symp. Digital Signal Process.*, London, U.K., July 1996.
[16] A. Papandreou, "Parameter estimation of noisy hyperbolic impulses using phase information," Tech. Rep. 0594-0001, Univ. Rhode Island, Kingston, May 1994.
[17] A. Papandreou, S. M. Kay, and G. F. Boudreaux-Bartels, "The use of hyperbolic time-frequency representations for optimum detection and parameter estimation of hyperbolic chirps," in *Proc. IEEE-SP Int. Symp. Time-Freq. Time-Scale Anal.*, Philadelphia, PA, Oct. 25–28, 1994, pp. 369–372.
[18] S. Peleg and B. Porat, "Estimation and classification of signals with polynomial phase," *IEEE Trans. Inform. Theory*, vol. 37, pp. 422–430, 1991.
[19] B. Porat, *Digital Processing of Random Signals, Theory, and Methods.* Englewood Cliffs, NJ: Prentice-Hall, 1994.
[20] B. Porat and B. Friedlander, "Blind deconvolution of polynomial phase signals using the high-order ambiguity function," *Signal Process.*, vol. 53, pp. 149–163, 1996.
[21] A. W. Rihaczek, *Principles of High-Resolution Radar*. San Diego, CA: Peninsula, 1985.
[22] S. Shamsunder, G. B. Giannakis, and B. Friedlander, "Estimating random amplitude polynomial phase signals: A cyclostationary approach," *IEEE Trans. Signal Processing*, vol. 43, pp. 492–505, Feb. 1995.
[23] P. Sircar and S. Sharma, "Complex FM signal model for nonstationary signals," *Signal Process*, vol. 57, pp. 283–304, 1997.
[24] F. G. Stremler, *Introduction to Communication Systems*, 3rd ed. Reading, MA: Addison Wesley, 1990.
[25] A. Swami, "Cramér–Rao bounds for deterministic signals in additive and multiplicative noise," *Signal Process.*, vol. 53, pp. 231–244, 1996.
[26] G. T. Zhou, G. B. Giannakis, and A. Swami, "On polynomial phase signals with time-varying amplitudes," *IEEE Trans. Signal Processing*, vol. 44, pp. 848–861, Apr. 1996.
[27] G. T. Zhou and G. B. Giannakis, "Parameter estimation of FM signals using cyclic statistics," in *Proc. IEEE-SP Int. Symp. Time-Freq. Time-Scale Anal.*, Philadelphia, PA, Oct. 25–28, 1994, pp. 248–251.
[28] J.-E. Wilbur and R. J. McDonald, "Nonlinear analysis of cyclically correlated spectral spreading in modulated signals," *J. Acoust. Soc. Amer.*, vol. 92, pp. 219–230, July 1992.

Fulvio Gini was born in Fuecchio, Italy, on February 25, 1965. He received the Doctor Engineer (cum laude) and the Research Doctor degrees in electronic engineering from the University of Pisa, Pisa, Italy, in 1990 and 1995, respectively.

He is currently a Tenured Research Fellow at the "Dipartimento di Ingegneria dell'Informazione," University of Pisa. From July 1996 to January 1997, he was a Visiting Researcher with the Department of Electrical Engineering, University of Virginia, Charlottesville. His general interests are in the areas of statistical signal processing, estimation, and detection theory. In particular, his research interests include non-Gaussian signal detection and estimation using higher order statistics, cyclostationary signal analysis, and estimation of nonstationary signals, with applications to radar and digital communications.

Georgios B. Giannakis (F'96) received the Diploma degree in electrical engineering from the National Technical University of Athens, Athens, Greece, in 1981. From September 1982 to July 1986, he was with the University of Southern California (USC), Los Angeles, where he received the M.Sc. degree in electrical engineering in 1983, the M.Sc. degree in mathematics in 1986, and the Ph.D. degree in electrical engineering in 1986.

After lecturing for one year at USC, he joined the University of Virginia (UVA), Charlottesville, in 1987, where he became a Professor of Electrical Engineering in 1997, and Graduate Committee Chair and Director of the Communications, Controls, and Signal Processing Laboratory in 1998. Since January 1999, he has been with the University of Minnesota, Minneapolis, as a Professor of Electrical and Computer Engineering. His general interests lie in the areas of signal processing and communications, estimation and detection theory, time-series analysis, and system identification; he has published more than 90 journal papers on these subjects. Specific areas of expertise include (poly)spectral analysis, wavelets, cyclostationarity, and non-Gaussian signal processing with applications to SAR, array, and image processing. Current research topics focus on transmitter and receiver diversity techniques for equalization of single-user and multiuser communication channels, mitigation of fading, compensation of nonlinear effects, redundant filterbank transceivers for block communications, and multicarrier and wideband communications systems.

Dr. Giannakis was awarded the School of Engineering and Applied Science Junior Faculty Research Award in 1988 and the EE Outstanding Faculty Teaching Award in 1992 during his 12 years with UVA. He received the IEEE Signal Processing Society's 1992 Paper Award in the Statistical Signal and Array Processing (SSAP) area. He co-organized the 1993 IEEE Signal Processing Workshop on Higher Order Statistics, the 1996 IEEE Workshop on Statistical Signal and Array Processing, and the first IEEE Signal Processing Workshop on Wireless Communications in 1997. He guest coedited two Special Issues on high-order statistics (*International Journal of Adaptive Control and Signal Processing*, and the EURASIP journal *Signal Processing*) and the January 1997 *Special Issue on Signal Processing for Advanced Communications* of the IEEE TRANSACTIONS ON SIGNAL PROCESSING. He has served as an Associate Editor for the IEEE TRANSACTIONS ON SIGNAL PROCESSING and the IEEE SIGNAL PROCESSING LETTERS, a secretary of the Signal Processing Conference Board, a member of the SP Publications board, and a member and Vice-Chair of the SSAP Technical Committee. He now chairs the Signal Processing for Communications Technical Committee. He is also a member of the IMS and the European Association for Signal Processing.